REMARK: Please find in the following our response to the referees comments. In addition to this official review we revised the manuscript in response to a personal communication reaching use after the discussion period was closed. Our response to the latter can be found afterwards.

<mark>**All line numbers refer to the manuscript with marked changes.**</mark>

<u>Referee #1:</u>

This manuscript describes the implementation of a terrestrial phosphorus cycle into the land surface model ORCHIDEE. The authors used the fertilization experiments at two sites along the Hawaii chronosequence to evaluate the nutrient representation in the NP-enabled ORCHIDEE. With the increasing realization of the important role of phosphorus cycle in affecting global carbon cycle, this work is timely. Overall the manuscript is well written as a modelling paper. I just have some suggestions and edits as shown below.
DSG: We thank the referee very much for his constructive comments on our work.

General comments:
1) Introduction a bit too short – maybe it is sufficient for a modeling paper on GMDD but I think a bit more on how this representation of P cycle is different from other P models will position this work better
DSG: We fear a fruitful discussion of existing model concepts would make the introduction very long and distract from the the main scope. Nonetheless, we added a sentence to the introduction to stress the novel concepts we developed here: "It is the first global phosphorus models which explicitly simulates root uptake of dissolved phosphorus accounting for soil moisture effects on soil phosphorus mobility."

2) I would like to see a model diagram that shows the phosphorus pools and fluxes and maybe with major phosphorus processes. Although those have been described here and there in the manuscript, a diagram will help the reader to better understand the model and link them with many equations in the text.
DSG: We added a Figure (Figure 1) with pools and fluxes of the phosphorus cycle.
3) Figure 2 seems a repetition of a subcomponent of Figure 1 and can be emoved,
DSG: We removed Figure 2.
4) Labile phosphorus was used in the text to describe both labile phosphorus in plant and soils and it can be confusing sometimes.

DSG: we now consistently use 'soil labile phosphorus' / 'dissolved labile phosphorus' for labile P in soils and 'plant labile phosphorus' for labile P in plants throughout the text.

Minor comments:

Page 2, line 10: change "rise" to "rises"

DSG: corrected

Page 2, lines 22-25: acronyms were used (Ama, Euc, IMB, AFE......), not sure what they are and no references for them

DSG: these are abbreviations are due to the latex citation style file. This will be corrected with the help of the typsetter at a later stage.

Page 3, line 20: should be "except for"

DSG: corrected

Page 3, eq. 2: is this eq. complete?

DSG: equation was incorrect. we corrected the equation

Page 4, lines 12-14: this is not clear to me

DSG: we rephrased the text to

"As the concentration of phosphorus in roots is orders of magnitudes larger than the concentration in the soil solution, passive uptake of phosphorus via diffusion is negligible (Schachtman et al., 1998). Thus, only active uptake via specialized transporters on the root surface is accounted for in the model."

Page 5, eq. 3: umax – maximum root uptake capacity and vmax ->maximum uptake capacity of roots. Seems the same thing to me – need to be better defined. Also, I could not get the units on the two sides of the eq. consistent

DSG: equation was incorrect. we corrected the equation

Page 6, line 22: " the actual value of fPNplant may be higher than 1" – what is the implication for plant P uptake? Is it realistic?

DSG: This is the justification for the min() in the equation which was missing. we corrected the equation

Page 8, eq 12: how C growth is scaled? Photosynthesis or NPP? Equation will be helpful here

DSG: we added the equation EQ13

Page 9, section 2.1.3: This section is very general – not P specific. Could be removed or make it more focusing dynamics in litter and soil organic matter

DSG: The phosphorus dynamics in litter and soil organic matter follow the original model. We report the general concepts here. We would like to the keep this section for completeness, but can remove it to the appendix if the editor thinks this is needed.

Page 9, line 27: the turnover time of phosphorus is set to half the turnover times used for biological mineralization of organic matter – what is based on? Or Any reference?

DSG: We added "are set arbitrarily, due to the lack of observational constraints,"

Page 10, line 2: from primary minerals

DSG: corrected

Page 11, eq 27: should it be the other way around? When diffusion flux is greater than uptake, there is no change in the difference in labile P between root surface and the surrounding

DSG: corrected

Page 12, section 2.1.7: this section only deals with N fixation – can be put in appendix if needed

DSG: moved to appendix

Page 12, section 2.1.8:

DSG: ?

Page 19, line 6: should be "due to"

DSG: corrected

Page 20, Table 4: I feel the comparison between simulated and observed can be better shown with a chart instead of a table

DSG: we prefer to show the results in a table. no changes done.

Page 20, lines 8-10: I thought the PFT used here is tropical evergreen instead of tropical deciduous

DSG: this is just the phenology, there is still climate(drought) related mortality

Page 24, Line 14-15: foliar P concentration is much more variable than N concentration, could it be due to that the pre-defined foliage P concentration range is too narrow?

DSG: The leaf N:P range is prescribed from data from a global plant trait database with extensive data coming from nearby location. Thus the confidence is high, however the concepts applied to adjust stoichiometry itself are problematic and a cause of the mismatch between observed and simulated adjustments. Thus we added: "However, the stoichiometric adjustments in ORCHIDEE are not process-based and might be itself the cause for the bias in the simulated response of leaf stoichiometry."

Personal communication / Referee #2:

Comment on "A representation of the phosphorus cycle for ORCHIDEE" by D. S. Goll et al.

The manuscript by Goll et al. describes a new representation of phosphorus (P) cycle in theORCHIDEE model. The authors use observed data from two hronosequence, fertilization experiments in Hawaii to calibrate and evaluate the model. The impact of nutrients has been shown to be very important to global carbon cycle under climate change and increasing CO2 in many independent studies. The introduction of P cycle in land carbon models helps to improve our understanding on

how P interacts with carbon (C) and nitrogen (N) cycles and thus associated future climate change. Therefore, the manuscript is in the scope of Geoscientific Model Development. Nevertheless, there are several issues which
need to be addressed.

DSG: We thank the referee very much for is constructive and in depth comments on our work. We believe they substantially improved the quality of our work.
<mark>All line numbers refer to the manuscript with marked changes.</mark>

Major comments:

1. The manuscript presents a new P cycle parameterization added in a C-N cycle coupled land surface model, but it is not clear what the difference is in C/N cycle when P cycle is implemented in comparison with the original C-N model. A quantity analysis on C, N pools and fluxes with and without P cycle would be easier for readers to follow the impacts of P inclusion in the model. The authors only present results from the P model simulation. It would be important to show that including P cycle at least does not degrade the simulation by model with just N limitation.

DSG: The structure of the model does not allow to turn on/off the nutrient cycles in a straightforward way like it is possible with simpler models like CLM (Yang et al., 2014) or JSBACH (Goll et al., 2012) in which phosphorus affects carbon fluxes only via a minimum law. Technically we can run the model assuming an optimal nutrient availability, but these simulations deviate strongly from the observation as indicated by the strong simulated response to nutrient addition at the two sites presented here.

The rationale behind the nutrient manipulation experiment presented here is to evaluate the nutrient cycle and their effect on plant biomass and productivity. As stated in the introduction (Page2, L15-21), it is shown and now widely accepted in the community that manipulation experiment are best suited to evaluate the structure of a model. We therefore do not see much advantage of presenting simulation in a carbon only mode (assuming this would be technically feasible which it isn't).

No changes to the manuscript.

2. The length corrected spin-up seems problematic to me because it assumes that the model is able to reproduce the evolution of land ecosystem before its equilibrium state, but usually it is not the case. Most commonly spin-up consist of initializing both physical and   biogeochemical variables before running the model to equilibrium. The

integration time needed by the model to converge towards its own attractor is different from the true state of the natural ecosystem (Séférian et al. 2016). So the 300yr model period during spin-up should not be treated as the 300yr actual time of natural system. I may drop the way in Appendix B and (1) run the model until the C, N and P pools comparable to observed values (Table2, Crews et al. 1995), (2) ensure that the carbon accumulation rate in vegetation and soil fall in the range of the ~10yr observation. This ensures that the model state is comparable to the true state at the end of spin-up, which is required by starting the fertilization experiment.

DSG: We agree with the referee that these model might not be able to reproduce the pace at which land ecosystem converge towards its equilibrated state.

As a response to the referees concerns, we show the evolution of NPP, total biomass, total soil organic matter during the spinup simulation in Figure R1. The simulated variables for the year 234 (which correspond to the first year of climatic forcing period) are closest to the observation (Figure R1). This year is very close to the length of 230 yr we deduced from nitrogen accumulation estimates.

Due to the small differences, we prefer to keep the 230 yr length. The good agreement of simulated and observed carbon fluxes and stocks shows that the model is, despite we cannot assume such behaviour per se as the referee stated, able to capture the state of the ecosystem (Figure 3 & Table 4).

We state this more clearly now (P30,L19):
"As the simulated NPP , biomass, and soil organic matter match the observation (Table 4) and the dynamically simulated BNF rates are with 2.25 g(N)m−2 yr−1 well within the observed range, the reduction of the simulation length seems appropriate."
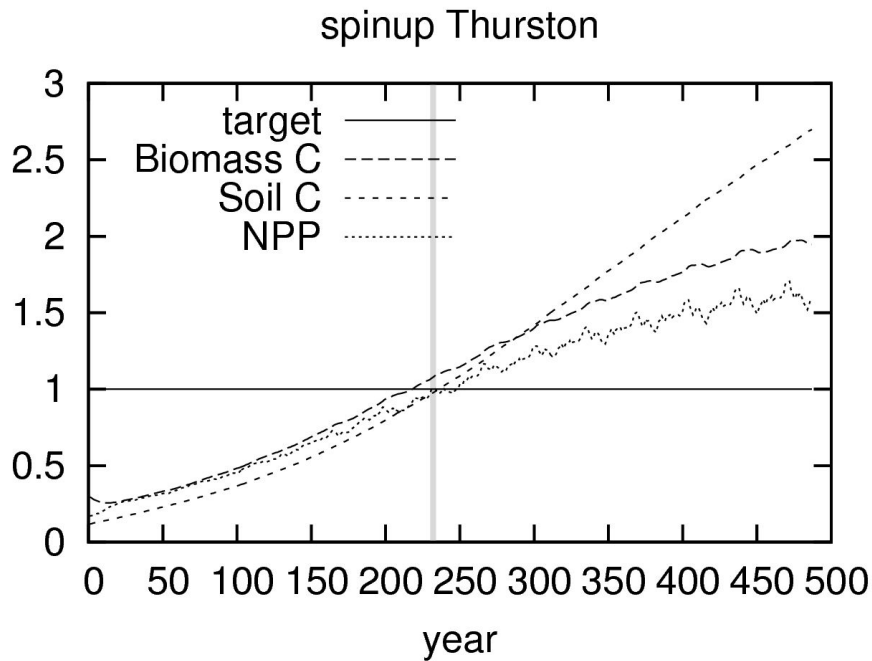
spinup Thurston

Figure R1: Net primary productivity, total biomass, and soil organic matter during the spinup simulation. Shown are 30yr running averages of simulated values divided by the observation flux of pool for the site. If the variables equals 1 it means simulated and observed variables are equal.

3. It is worthy of looking at why there is so large interannual variability of NPP as simulated by the model. Figure 3 shows that compared to the observation, the interannual variability of NPP is much higher than observations at both the N-limited and P-limited sites. This implies there must be some parameters or processes too sensitive to model forcing. A sensitivity analysis would help improve the understanding of the model dynamics. The authors attribute the larger interannual variability of the 4.1Myr site to an amplification of the drought induced growth reduction under low P availability. It is not very convincing because it only shows monthly values within a single year (Figure A1). However fluxes with large monthly variability do not necessarily combine to fluxes with strong interannual variability. I am wondering why the authors not present the annual results to sddress this issue directly?

DSG: We agree with the referee about the shortcomings of our analysis. However, a detailed analysis of the inter-annual variability would blow up the manuscript to an extent we fear the main points we make with this work would be diluted. Hereby, the lack of any information about the interannual variability of the two Hawaii site poses a big problem. We thus remove this analysis and will address the interactions of phosphorus limitation and interannual variability of NPP using an appropriate observational dataset in a follow up study.

4. It is unclear what processes are responsible for the occurrence of the N limitation at the 300yr site and the P limitation at the 4Myr site. Further analysis and discussion is missing to clarify why the model simulates contrasting responses to the same fertilization treatment at the N-limited and P-limited sites as shown in Figure 4. **DSG: We adjusted our simulation setup so that the only differences between the two sites are a) organic matter accumulation rate, b) phosphorus inputs, c) labile phosphorus sorption. Thereby, the changes in the N vs P limitation is solely an outcome of the different soil development stages following the classical concept by Walker and Syres (1976).**

We modified the method section accordingly (P15,L25-30): *"We account for changes in the sorption characteristics of volcanic soils are they develop. For the 300\unit{yr} site, we use the average value of k_s for Andisols from \citep{Yang2011}. For the 4.1\unit{Myr} site k_s was scaled with the relative difference in soil phosphorus sorption capacity between the two sites as computed dynamically in the P-enabled version (Violette in prep) of the mechanistic weathering model WITCH \citep{Godderis2006}."*

All values in text, tables and figure were updated with the simulated value from the new simulation. We took advantage of our recent code developments and use a newer revision of ORCHIDEE (r4520).

We now explicitly state in the discussion the mechanism resulting in the contrasting nutrient availabilities (which are now reported in Table 4):

(P21,L7-14): *"The differences in stoichiometry mirror differences in the respective availabilities of mineral nitrogen and soil labile phosphorus (Table~\ref{tab:results}). While the concentration of mineral nitrogen is extremely low at the young site due to a high immobilization demand of accumulating soil organic matter, the concentration is high at the old site where immobilization demand is met by the mineralisation of nitrogen from organic matter. In case of phosphorus, the high phosphorus input of 434. \unit{mg m^{-2} yr^{-1}} at the 300\unit{yr} site keep soil labile phosphorus concentration high despite the high immobilization demand. At the the old site, the extremely low phosphorus inputs of 0.27 \unit{mg m^{-2} yr^{-1}} result in low soil labile phosphorus concentration as the ecosystem relies primarily on the mineralisation of phosphorus from soil organic matter. "*

and

(P22/23): *"The 300\unit{yr} site is accumulating organic material, in particular soil organic matter, and the accompanied immobilization of soil nutrients is the major driver of nutrient scarcity. This leads to extremely low mineral nitrogen concentration. whereas the high weathering release of phosphorus from minerals is sufficient to keep soil labile phosphorus concentration relatively high (Table~\ref{tab:results}). Therefore, vegetation reacts strongly to the addition of nitrogen at the young site. The lack of any stimulation of plant productivity in the model to phosphorus addition at the young site indicates an overestimation of plant available phosphorus likely due to the omission of differences in the occlusion rate of soil labile phosphorus among sites which tends to be much higher at the young site (Violette in prep). At the 4.1\unit{Myr} site the remobilization of phosphorus from soil organic matter is the major source of phosphorus for vegetation, as the minerals are phosphorus depleted leading to low soil labile phosphorus concentration Table~\ref{tab:results}). Compared to the young site, also a higher fraction of soil labile phosphorus is adsorbed to soil particles and thus not available to plants. Therefore, vegetation reacts strongly to the addition of phosphorus at the old site, but not to nitrogen addition."*

5. Section 2.2.3: I would prefer to compare Xuptake and Xcontent with observations instead of using the derived values XUE, and Xprod and XMRT. Simpler analysis would be more straightforward and easier to understand the model's P cycle parameterization.
DSG: we agree that this variables are interesting and added the simulated values to Table 4.

Minor:
P2 L23-24: Abbreviations in the text should be written out (for example Ama; Euc; IMB;
AFE).
DSG: these are abbreviations are due to the latex citation style file. This will be corrected with the help of the typsetter at a later stage.
Section 2.1.1: The parameterization of the relationship between leaf nitrogen concentration
and Vcmax needs improvement with mathematical descriptions.
- What is the relationship between Nleaf, Nleaf,h*, Nstr Please clarify using formulas.
DSG: We added equation 2 (P3,L30)
Eq2 seems incomplete, what assumption is used for correction with Nstr?
- Missing is the description of how Jcmax is parameterized.
DSG: We already state in the text (P4,L1-2) *"The electron transport capacity ($J_{max,h}$) is derived from $V_{cmax,h}$ using the relationship from*

\citet{Kattge2007} which accounts for acclimation of photosynthesis to monthly temperatures." **See original publications for equations. No changes to manuscript.**

P5, Eq.3: The unit of the function not equal to g(P)g-1 (C)t-1

DSG: We corrected equation (Eq.4, P5)

P7, Eq.8: Representation of function needs recheck. Same parameterization for different

conditions?

DSG: We corrected the equation (Eq.9,P6)

Missing is the function of ftemp in Eq.6, and LF in Eq. 13, and the values of parameter gmax

in Eq.11.

DSG: We added the equation 5 for ftemp and added the value of gmax in Table 2. We already give the reference of how LF is calculated (P8,L3-5) . We think this is sufficient as this variables is independent of the nutrient cycles.

P9, Eq. 17: [...] is missing and should be added in Table A1.

DSG: We added the value to Table 2.

P10, Eq. 20: I assume the sign of [...] in the function should be negative as [...]. Please describe briefly the difference between [...] and [...] To make the text more readable, details of each components in Eq.20 should be described briefly with functions if possible.

DSG: We corrected the equation (Eq21,P10) and description of components were added with references to the respective equations (P10,L5-6).

P21, L11: Edit: Foliage N:P ratios less than 14…

DSG: corrected

P31, L21: typo? Should be "-44.7%" here.

DSG: corrected

Section 2.1.8: How the quality of Litter and SOM affects nutrient availability? A brief description of P immobilization and mineralization with equations would help readability.

DSG: We already refer to the original publications describing the dynamics of decomposition, which were not modified. We prefer to keep the model description focused on the novel aspects. No changes to the manuscript.

Table 1. Could the unit "30minutes-1" be replaced by "t-1

" according to the definition of "t" in Table 2?

DSG: corrected

the unit g(dryweight) should be converted to g(C) for consistency.

DSG: corrected; also units of parameter r_d in Table2.

Table 2. For parameters [...]

 represents a unit by volume? Please clarify.

DSG: we corrected equation (Eq4, P5).

Table 3. The 300yr site should be "Kokee" but not "Koke".
DSG: corrected throughout the manuscript
Fig 1. Adding a schematic representation of model structure as Yang et al. (2014) would be
beneficial for readers to understand the whole picture of the model.
DSG: we added a flowchart of the P cycle (Figure 1)

Fig 2. Duplicated information with Figure 1 but the rational very useful for explaining how nutrients affect plant production in the model. Better to move to the part of discussion and calculate the values of pools and fluxes to explain the different responses to N/P fertilization as shown in Fig4.
DSG: It is not straightforward to quantify the feedbacks from the simulation we performed as the different processes operate on different timescales. To avoid the redundant information we remove this figure.

Reference:
Séférian et al. 2016, Inconsistent strategies to spin up models in CMIP5: implications for
ocean biogeochemical model performance assessment.

A representation of the phosphorus cycle for ORCHIDEE (revision 3985 4520)

Daniel S. Goll[1], Nicolas Vuichard[1], Fabienne Maignan[1], Albert Jornet-Puig[1], Jordi Sardans[2,3], Aurelie Violette[4], Shushi Peng[6], Yan Sun[6], Marko Kvakic[7], Matthieu Guimberteau[1,8], Bertrand Guenet[1], Soenke Zaehle[5], Josep Penuelas[2,3], Ivan Janssens[9], and Philippe Ciais[1]

[1]Le Laboratoire des Sciences du Climat et de l'Environnement, IPSL-LSCE CEA/CNRS/UVSQ Saclay, Gif sur Yvette, France.
[2]CSIC, Global Ecology Unit CREAF-CSIC-UAB, 08193 Bellaterra, Catalonia, Spain
[3]CREAF, 08193 Cerdanyola del Vallés, Catalonia, Spain
[4]LMTG - Laboratoire des Mécanismes et Transfert en Géologie, Toulouse, France.
[5]Biogeochemical Integration Department, Max Planck Institute for Biogeochemistry, Jena D-07701, Germany
[6]Sino-French Institute for Earth System Science, College of Urban and Environmental Sciences, Peking University, Beijing 100871, China
[7]ISPA, Bordeaux Sciences Agro, INRA, 33140 Villenave d'Ornon, France
[8]Sorbonne Universités, UPMC, CNRS, EPHE - UMR7619 METIS, 75252 Paris, France
[9]Department of Biology, University of Antwerp, Universiteitsplein 1, 2610 Wilrijk, Belgium

Correspondence to: Daniel S. Goll (daniel.goll@lsce.ipsl.fr)

Abstract. Land surface models rarely incorporate the terrestrial phosphorus cycle and its interactions with the carbon cycle, despite the extensive scientific debate about the importance of nitrogen and phosphorus supply for future land carbon uptake. We describe a representation of the terrestrial phosphorus cycle for the land surface model ORCHIDEE, and evaluate it with data from nutrient manipulation experiments along a soil formation chronosequence in Hawaii.

5   ORCHIDEE accounts for influence of nutritional state of vegetation on tissue nutrient concentrations, photosynthesis, plant growth, biomass allocation, biochemical (phosphatase-mediated) mineralization and biological nitrogen fixation. Changes in nutrient content (quality) of litter affect the carbon use efficiency of decomposition and in return the nutrient availability to vegetation. The model explicitly accounts for root zone depletion of phosphorus as a function of root phosphorus uptake and phosphorus transport from soil to the root surface.

10   The model captures the observed differences in the foliage stoichiometry of vegetation between an early (300yr) and a late stage (4.1 Myr) of soil development. The contrasting sensitivities of net primary productivity to the addition of either nitrogen, phosphorus or both among sites are in general reproduced by the model. As observed, the model simulates a preferential stimulation of leaf level productivity when nitrogen stress is alleviated, while leaf level productivity and leaf area index are stimulated equally when phosphorus stress is alleviated. The nutrient use efficiencies in the model are lower as observed

15   primarily due to biases in the nutrient content and turnover of woody biomass.

We conclude that ORCHIDEE is able to reproduce the shift from nitrogen to phosphorus limited net primary productivity along the soil development chronosequence, as well as the contrasting responses of net primary productivity to nutrient addition.

1 Introduction

As it has been acknowledged that human activity is changing Earth's climate, it is argued that climate research needs to sharpen its view (Marotzke et al., 2017). At it's new suggested focus is the fate of the emitted carbon which is closely linked to the extensive scientific debate about the importance of nutrient limitation (nitrogen and phosphorus supply) for future land carbon uptake (for example Peñuelas et al. (2013); Wieder et al. (2015); Brovkin and Goll (2015)). Yet, none of the earth system models (ESM), which are major tools in advancing the understanding of the role of human activities in the climate system, incorporate a terrestrial phosphorus cycle.

The few existing land surface models (LSM) which account for interactions between phosphorus availability and the land carbon cycle suggest a significant role of phosphorus availability for ecosystems on highly weathered soils (Wang et al., 2010; Goll et al., 2012; Yang et al., 2014) with increasing significance as carbon dioxide concentration ~~rise~~ rises (Goll et al., 2012). However, these findings are highly uncertain due to processes which are poorly constrained by current observational data: soil phosphorus sorption dynamics, phosphatase-mediated mineralization, stoichiometric plasticity, leaf nutrient recycling, and the effects of phosphorus limitation on vegetation (photosynthesis, growth, allocation, mortality) (Wang et al., 2010; Goll et al., 2012; Yang et al., 2014; Reed et al., 2015).

Ecosystem manipulation experiments are shown to provide useful information to assess and evaluate LSMs (Medlyn et al., 2015; Meyerholt and Zaehle, 2015), which, in return, facilitate the interpretation of observation data and can guide the design of experiments (Medlyn et al., 2015). The long-term (6–10 years) fertilization experiment in a soil formation chronosequence in Hawaii (Harrington et al., 2001; Ostertag, 2001), with its contrasting availabilities of nitrogen and phosphorus along a soil age gradient going from young phosphorus-rich and nitrogen-poor soils to old highly-weathered soils low in phosphorus but rich in nitrogen, provides an ideal test case for the evaluation of nutrient component in LSMs (Wang et al., 2007; Yang et al., 2014).

The potentially important influence of phosphorus availability on the land carbon balance and the recently initiated ecosystem scale manipulation experiments in phosphorus poor environments (for example Ama; Euc; IMB; AFE) as well as other projects related to the role of phosphorus in ecosystem functioning (for example, SPP; QUI) call for the need of new phosphorus enabled LSMs to keep track with these actions (Reed et al., 2015).

Here, we describe the implementation of the terrestrial phosphorus cycle into the LSM ORCHIDEE (Krinner et al., 2005) following the principles developed earlier for the introduction of the nitrogen cycle into ORCHIDEE (Zaehle and Friend, 2010). It is the first global phosphorus models which explicitly simulates root uptake of dissolved phosphorus accounting for soil moisture effects on soil phosphorus mobility. The model is then evaluated with data from a long-term fertilization experiment in a soil formation chronosequence in Hawaii (Harrington et al., 2001; Ostertag, 2001).

2 Methods

2.1 Model description

The land-surface model used for this study ORCHIDEE, is based on two different modules (Krinner et al. (2005), their Fig. 2). The first module describes the fast processes such as the soil water budget and the exchanges of energy, water and CO_2 through photosynthesis between the atmosphere and the biosphere. The second module simulates the carbon dynamics of the terrestrial biosphere and essentially represents processes such as maintenance and growth respiration, carbon allocation, litter decomposition, soil carbon dynamics and phenology. Global vegetation is described by 13 meta-classes which correspond to plant functional types (PFT) with a specific parameter set (one for bare soil, eight for forests, two for grasslands and two for croplands).

The major modification since Krinner et al. (2005) are listed in the following: a slightly revised carbon allocation scheme from a recent side branch of ORCHIDEE (Naudts et al., 2015), which avoids the capping of leaf area index at a predefined value; an explicit representation of mesophylic conductance to CO_2 and omission of direct effects of soil moisture stress on the maximum rate of carboxylation (V_{cmax}) (Vuichard in prep); a revised thermodynamic scheme which accounts for the heat transported by liquid water into the soil, in addition to the heat conduction process (Wang et al., 2016).

2.1.1 Starting version

The implementation of the phosphorus (P) cycle into ORCHIDEE was done into the nitrogen enabled version of ORCHIDEE (ORCHIDEE-CN) (Vuichard in prep.). ORCHIDEE-CN is a re-implementation of the nitrogen cycle from a discontinued version of ORCHIDEE (which became OCN (Zaehle and Friend, 2010; Zaehle et al., 2011)) into a recent version of ORCHIDEE (r3623). The nitrogen cycle in OCN is well evaluated (De Kauwe et al., 2014; Zaehle et al., 2014; Walker et al., 2015; Meyerholt and Zaehle, 2015) and identical to the one in ORCHIDEE-CN except for the parametrization of the relationship between leaf nitrogen concentration and maximum carboxylation capacity of photosynthesis (V_{cmax}) as ORCHIDEE (r3623) uses a different carbon assimilation scheme than originally used in Zaehle and Friend (2010). V_{cmax} is directly derived from the leaf nitrogen concentration at the respective canopy level following Kattge et al. (2009):

$$V_{cmax,h} = nue N^*_{leaf,h} \tag{1}$$

where $N^*_{leaf,h}$ is nitrogen concentration in leaves at canopy level (h). $N^*_{leaf,h}$ is derived from nitrogen in leaf biomass per ground area (N_{leaf}) using an exponential canopy nitrogen profile (Johnson and Thornley, 1984). $N^*_{leaf,h}$ is corrected for a certain fraction of structural nitrogen per leaf carbon (N_{str}) which does not contribute directly to the carboxylation capacity of photosynthesis (Table 2).

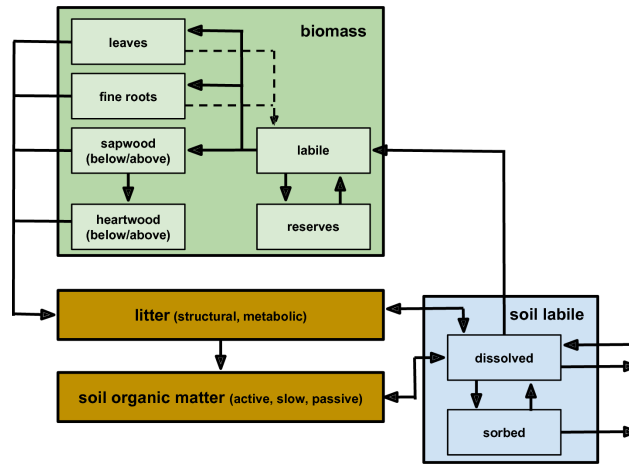$$N^*_{leaf,h} = (N_{leaf} - N_{str}) exp(-\kappa_N h) \tag{2}$$

Figure 1. Pools and fluxes of the phosphorus component of ORCHIDEE.
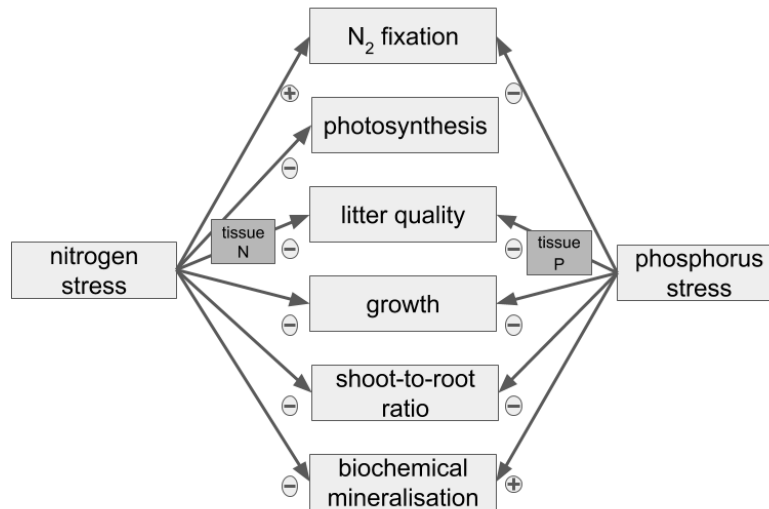

Figure 2. The effects of nitrogen and phosphorus stress (sub-optimal internal availability) on vegetation and associated processes in OR-CHIDEE. A shortage of internal nutrients reduces tissue nutrient concentrations, overall growth (Equation 12), the shoot-to-root ratio of new growth (Equation 14), litter quality, and in case of nitrogen the carboxylation efficiency of photosynthesis (Equation 1). In addition, processes enhancing the availabilities of nitrogen and phosphorus are up regulated (Equation 18&B2).

where κ_N is the extinction coefficicent. The electron transport capacity ($J_{max,h}$) is derived from $V_{cmax,h}$ using the relationship from Kattge and Knorr (2007) which accounts for acclimation of photosynthesis to monthly temperatures.

In the following the representation of the terrestrial phosphorus cycle and its interaction with the cycles of carbon and nitrogen are described. All variables and parameter can be found in Table 1 and 2, respectively.

2.1.2 Vegetation: phosphorus uptake, allocation and turnover

Vegetation biomass (carbon, nitrogen and phosphorus) is separated into leaves, roots, sapwood, heartwood, short-term (labile) and long-term storage (reserves) (Zaehle and Friend, 2010; Naudts et al., 2015) (Figure 1). We prescribed boundaries for the stoichiometry of leaves, roots, sapwood, heartwood, but not for labile and reserves (Table A1) (Zaehle and Friend, 2010).

5   Plants take up labile ~~dissolved phosphorus from the soil solution~~ phosphorus dissolved in soil solution (solution phosphorus) following the representation of root nitrogen uptake (Zaehle and Friend, 2010). Plant nutrient uptake is simulated as a function of mineral nutrient availability with the aim to account for the increase in uptake in nutrient starved plants by increasing the uptake capacity per root surface (Schachtman et al., 1998), as well as indirectly through increased root growth and exploration of the soil by roots to increase their resource acquisition (Schachtman et al., 1998). Mycorrhizae are implicitly included

10   in root biomass as mycorrhizal hyphae show comparable uptake characteristics as roots (Schachtman et al., 1998). ~~Due to major contribution of active uptake relative to passive uptake by water flow, we omit to explicitly simulate passive uptake (Schachtman et al., 1998).~~ As the concentration of phosphorus in roots is orders of magnitudes larger than the concentration in the soil solution, passive uptake of phosphorus via diffusion is negligible (Schachtman et al., 1998). Thus, only active uptake via specialized transporters on the root surface is accounted for in the model. Hereby, the model does not distinguish between

15   organic and inorganic forms of dissolved labile phosphorus.

The ~~maximum~~ x root uptake capacity (u_{max}) per root mass (C_{root}) for a given solute concentration follows the combined behavior of low-affinity and high-affinity transporter systems working in parallel which typically shows no saturation at high soil solute concentrations (Kronzucker et al., 1995; Zhang et al., 2009) and is given by:

$$u_{max} = v_{max} a_{root} P_{sol} \left(\frac{k_{Pmin}}{c_k} + \frac{1}{P_{sol} + c_k K_{Pmin}} \right) \tag{3}$$

20   where v_{max} is the maximum uptake capacity, $a_{root} \frac{P_{sol}}{\Theta}$ is the dissolved labile phosphorus concentration at the root surface (Equation 23), and c_k a unit conversion factor ~~to convert from phosphorus concentration per soil volume to phosphorus per ground area (P_{sol})~~ using the soil type specific parameter for soil moisture content at saturation in ORCHIDEE (mcs) as an approximation of pore space following Smith et al. (2014).

The combined behavior of the two uptake systems is approximated by the term in brackets, where the linear factor (k_{Pmin})

25   was chosen to match the observed rate of increase in overall phosphorus uptake at high dissolved labile phosphorus concentration (low affinity transporter) (Zhang et al., 2009) (Table 2). The values for the Michaelis-Menten constants are averages of the values reported in Schachtman et al. (1998) (page 448) for K_{Pmin} of the high-affinity system (Table 2). We initially used the values reported in Bouma et al. (2001) for v_{max} for orange trees, but had to reduce these value by a factor of 10 to achieve realistic uptake behavior (Table 2).

30   Plant uptake (F_{up}) is derived from multiplying the root uptake capacity with the root carbon mass (C_{root}) and is scaled with fPN_{plant} to account for actual phosphorus demand and with f_{temp} to avoid phosphorus accumulation in plants and soil at low temperature:

$$F_{up} = u_{max} C_{root} fPN_{plant} f_{temp} \tag{4}$$

The temperature scaling function (Zaehle and Friend, 2010) is given by:

$$f_{temp} = min(exp(0.069 * (T_{soil} - T_{soil,ref})), 1.0) \tag{5}$$

As phosphorus uptake is energetically costly (Schachtman et al., 1998), plant phosphorus uptake is down-regulated according to the P:N ratio of plant tissue (pn_{plant}) avoiding excessive uptake of phosphorus (luxury consumption) when tissue phosphorus concentration are at the prescribed maximum ($pn_{leaf,max}$):

$$pn_{plant} = \frac{P_{labile} + P_{leaf} + P_{root}}{N_{labile} + N_{leaf} + N_{root}} \tag{6}$$

The dependency of phosphorus uptake on pn_{plant} is described as:

$$fPN_{plant} = min(max(\frac{pn_{plant} - pn_{leaf,max}}{pn_{leaf,min} - pn_{leaf,max}}, 0.0), 1.0) \tag{7}$$

where $pn_{leaf,min}$ and $pn_{leaf,max}$ are the minimum and maximum foliage P:N ratios. Note that, because neither the nitrogen nor the phosphorus concentration in the plant labile phosphorus pool (P_{labile}) is constrained by a prescribed P:N ratio($pn_{leaf,min}$), the actual value of fPN_{plant} may be higher than 1.

Further we scale plant phosphorus uptake with a temperature function (f_{temp}). We use the same equation as is used to scale soil carbon decomposition (Krinner et al., 2005), phosphorus mineralization, biochemical mineralization (Equation 18) and nitrogen uptake and mineralization (Zaehle and Friend, 2010). The equation avoids the accumulation of phosphorus in plants or soils at low temperatures, mimicking the inhibition of biological processes when soils are frozen which is not explicitly represented in ORCHIDEE.

The phosphorus taken up by plants enters their labile phosphorus pool (P_{labile}) which dynamics are given by:

$$\frac{dP_{labile}}{dt} = F_{up} + \sum_{i=leaf,root} \tau_i f_{trans,i} P_i - G_P + F_{reserve} \tag{8}$$

where τ_i is the fraction of foliage or roots shed each time step, $f_{trans,i}$ is the fraction of phosphorus recycled and transferred to plant labile phosphorus before tissue is shed, G_P is labile phosphorus allocated to new biomass and $F_{reserve}$ is the flux to or from the long-term storage ($P_{reserve}$).

Following the dynamics of labile nitrogen (Zaehle and Friend, 2010), P_{labile} is limited to a maximum size $P_{labile,max}$ which is taken as the phosphorus required to allocate the entire labile carbon pool according to the current growth rate and the maximum foliage phosphorus concentration. Any excess labile phosphorus is transferred to $P_{reserve}$ and is mobilized again if the size of the labile phosphorus pool falls below $P_{labile,max}$:

$$F_{reserve} = P_{labile} - P_{labile,max} \tag{9}$$

Following the assumption regarding nitrogen concentration (Zaehle and Friend, 2010), the phosphorus concentration in newly grown plant tissue is assumed to depend directly on the phosphorus concentration in the plant labile pool, providing a link between tissue activity and plant labile phosphorus availability. Foliage phosphorus concentration changes are simulated explicitly, with the phosphorus content of non-foliage tissue varying in proportion to that of the foliage, as observed along

gradients of soil fertility (Heineman et al., 2016). The phosphorus required (G_P) to sustain the current growth (G_C) of new tissue can be therefore written as:

$$G_P = (\lambda_{leaf} f_{leaf} + \lambda_{root}(f_{root} + f_{fruit}) + f_{sap}\lambda_{sap})(1 + D_{leaf}) nc_{leaf} pn_{leaf} G_C \tag{10}$$

where the f_i are the fractions of carbon allocated to foliage ($i = leaf$), roots ($i = root$), fruits ($i = fruit$) and sapwood (stalks
5   for grass) ($i = sap$) which are calculated dynamically (Zaehle and Friend, 2010; Naudts et al., 2015), nc_{leaf} and pn_{leaf} are the nitrogen to carbon and the phosphorus to nitrogen ratio of current foliage, λ_i are the phosphorus to carbon allocation to tissue i relative to the phosphorus to carbon allocation to leaves ($\lambda_{leaf} = 1$), and D_{leaf} is an empirical elasticity parameter.

Analog to leaf nitrogen concentrations (Zaehle and Friend, 2010), the foliage phosphorus concentrations are a dynamic state-variables. If the plant labile phosphorus pool is not sufficient to maintain the current phosphorus concentration at the
10 current carbon growth rate G_C, the phosphorus concentration of newly grown leaf tissue is allowed to decrease relative to the concentration of existing foliage. Conversely, if plant labile phosphorus is larger than required, and the plant is not in the phase of flushing new foliage, P concentrations are allowed to increase.

To dampen day-to-day variations in tissue nutrient concentrations, such as at the beginning of the growing season an empirical elasticity parameter (D_{leaf}) is included. Meyerholt and Zaehle (2015) tested different assumption about the stoichiometric
15 flexibility in the OCN model and showed that stoichiometric flexibility is needed to reproduce observational data from fertilization experiments, however, they found the original formulation in OCN was too flexible. Vuichard et al (in prep.) revised the formulation of the dampening equation for the leaf nitrogen concentration which is also applied for the leaf phosphorus concentration:

$$D_{leaf} = \begin{cases} D_{max}(1 - exp[-(1.6\frac{1/pn_{leaf} - 1/pn_{leaf,min}}{1/pn_{leaf,max} - 1/pn_{leaf,min}})]) & \text{for } P_{labile} < G_P \\ D_{max} exp[-(1.6\frac{1/pn_{leaf} - 1/pn_{leaf,min}}{1/pn_{leaf,max} - 1/pn_{leaf,min}})] & \text{otherwise} \end{cases} \tag{11}$$

20 We adapted the dependency of biomass growth to plant labile nitrogen availability (Zaehle and Friend, 2010) for the dependency to plant labile phosphorus availability (Figure 2): If the plant labile phosphorus concentration in vegetation fails to match the P requirement of biomass carbon growth, the growth of plant tissue is reduced proportionally to match phosphorus availability in the plant labile pool:

$$p_{lim} = min(1.0, \frac{g_{max} P_{labile}}{G_P}) \tag{12}$$

25 where g_{max} is a unit-less scalar regulating the maximal daily fraction of P_{labile} allocated to growth, to avoid a complete depletion of P_{labile} at any given time-step. g_{max} is also used to regulate the allocatable fraction of labile carbon and labile nitrogen and it is a function of temperature (Naudts et al., 2015). G_P is the estimated amount of phosphorus needed to support growth.

C growth (G_C) is then scaled by the minimum of growth limitation factors derived from phosphorus availability (p_{lim}) and
30 nitrogen availability (n_{lim}) (see Equation 22 in SI of Zaehle and Friend (2010)):

$$G_C = G_C min(p_{lim}, n_{lim}) \tag{13}$$

7

Nutrient stress in general affects the ratio leaf to root portioning of new growth:

$$C_{leaf} = n_{scal} f_{LF} C_{root} \tag{14}$$

where f_{LF} is a function relating leaf mass to root mass based on the pipe theory (Shinozaki et al., 1964) as ~~originally~~ implemented by Zaehle and Friend (2010) ~~(see equation 10 in Naudts et al. (2015))~~ and recently updated by Naudts et al. (2015). n_{scal} is the actual nutrient stress factor and is derived from the minimum of the nitrogen ($n_{scal,N}$) and phosphorus ($n_{scal,P}$) stress scaling factor:

$$n_{scal} = min(n_{scal,N}, n_{scal,P}) \tag{15}$$

$n_{scal,P}$ is given by the deviation of the actual plant phosphorus concentration from the maximal leaf phosphorus concentration relative to carbon concentration:

$$n_{scal,P} = \frac{pc_{plant}}{pc_{leaf,ave}} \tag{16}$$

where $pc_{leaf,ave}$ is average of the maximum and minimum leaf phosphorus to carbon ratios ($pn_{leaf,min}, pn_{leaf,max}, nc_{leaf,min}$, and $nc_{leaf,max}$) and pc_{plant} the growing season average of the plant labile phosphorus to labile carbon concentration:

$$pc_{plant} = \frac{P_{labile} + P_{root} + P_{leaf}}{C_{labile} + C_{root} + C_{leaf}} \tag{17}$$

The calculation of $n_{scal,N}$ follows the calculation of $n_{scal,P}$ with the exception that the deviation of the actual plant nitrogen concentration from the maximal leaf nitrogen concentration relative to carbon concentration is used (Zaehle and Friend, 2010).

Turnover of biomass phosphorus follows strictly the turnover of each biomass pool as described in Krinner et al. (2005). The phosphorus fluxes are derived from the carbon fluxes and the corresponding stoichiometric ratios, subtracting a fixed fraction of the phosphorus which is resorbed and added to plant labile pool.

2.1.3 Litter & soil organic matter

The turnover of litter and soil organic matter follows the CENTURY model (Parton et al., 1993), which describes decomposition as a function of substrate availability, clay content, soil moisture and soil temperature. Organic matter is separated into structural and metabolic litter and three soil organic matter pools (fast, slow, passive) which differ in their respective turnover times with no vertical discretization. Due to the fast turnover of microbial communities, microbial biomass is assumed to be always adjusted to the availability of labile organic matter and is thus part of the fast soil organic matter pool. The model is described in detail elsewhere (Krinner et al., 2005; Zaehle and Friend, 2010). The nitrogen concentrations of decomposing material are assumed to vary linearly with soil mineral nitrogen content. Instead of applying a comparable (empirical) approach for the phosphorus concentration of decomposing material (Parton et al., 1993; Kirschbaum et al., 2003), the phosphorus concentrations varies mechanistically as a function of biochemical mineralization (Equation 18) (Wang et al., 2010; Goll et al., 2012; Yang et al., 2014).

2.1.4 Biochemical mineralization

Biochemical mineralization (phosphatases-mediated) decouples the mineralization of phosphorus partly from carbon decomposition and nitrogen mineralization (McGill and Cole, 1981). In contrast to "biological mineralization" of nitrogen and phosphorus, biochemical mineralization is not driven by the energy demand of microorganisms. Although phosphatase activity, which
5   is a qualitative measure for biochemical mineralization, is common in soils (Stewart and Tiessen, 1987), the quantification of the mineralization rates in the field is not yet possible.

We simulate biochemical (phosphatases-mediated) mineralization of phosphorus (F_{bcm}) with the aim to account for the observed increase in F_{bcm} when plants experience sub-optimal P-to-N availabilities as an approximation of the stoichiometric status of the whole ecosystem (Margalef et al (submitted)) including the effect of substrate availability on mineralization
10   (McGill and Cole, 1981)(Figure ??): .

$$F_{bcm} = fPN_{plant} f_{temp} \sum \tau_{x,ref} P_x \tag{18}$$

where $\tau_{x,ref}$ is the turnover time of phosphorus in soil organic matter pool x (P_x) and the two other variables are scaling functions: First, biochemical mineralization is scaled according to the P:N status of vegetation (fPN_{plant}) to account for the observed link between rizosphere phosphatase activity and plant nutritional status (Fox, 1992; Hofmann et al., 2016). Second,
15   it is scaled with the same equation used to scale mineralization and root uptake according to soil temperature. The values of $\tau_{x,ref}$ are set arbitrarily, due to the lack of observational constraints, to half the turnover times used for the "biological mineralization" of organic matter (Krinner et al., 2005), except for $\tau_{passive,ref}$ which set to zero to account for inaccessible phosphorus in stabilized nutrient rich organic matter (Tipping et al., 2016).

2.1.5 Soil mineral phosphorus

20   The release of phosphorus from primary minerals is the primary source of phosphorus for many terrestrial ecosystem. In this study, we prescribed site specific release rates (F_{weath}), but a dynamic phosphorus weathering routine is implemented in ORCHIDEE which is described in the appendix.

Leaching (F_{leach}) of dissolved phosphorus (P_{sol}) occurs in proportion to fraction of soil water (Θ) lost by sum of simulated drainage and surface runoff (q):

25    $$F_{leach} = P_{sol} \frac{q}{\Theta} \tag{19}$$

We assume that at each time step a fixed fraction (k_s) of dissolved labile phosphorus is adsorbed onto soil particles and the remaining fraction ($1 - k_s$) is dissolved. Instead of the commonly used Langmuir equation, we chose a linear approach for sorption, which works well for low soil phosphorus concentrations, which are common in most natural ecosystems (McGechan and Lewis, 2002). The calibration of the Langmuir equation for global application represent a major challenge as global datasets
30   on soil phosphorus content are limited (Yang and Post, 2011) and parameters cannot be derived with enough confidence. Given the high sensitivity of the dynamics of available phosphorus on the sorption dynamics, we choose a simple but sufficiently

constrainable approach. Thus the dynamics of sorbed labile phosphorus (P_{sorb}) are given by:

$$\frac{dP_{sorb}}{dt} = k_s \frac{dP_{sol}}{dt} \tag{20}$$

The dynamics of dissolved labile phosphorus (P_{sol}) are given by (see Appendix A in Goll et al. (2012) for details): ~~where~~

$$\frac{dP_{sol}}{dt} = (1 - k_s)(F_{weath} - F_{up} + F_{min} + F_{bcm} - \tau_{sorb}P_{sorb} - F_{leach}) \tag{21}$$

5   where F_{weath} (Eq. A1) is phosphorus release from primary minerals, F_{up} (Eq. 4) is phosphorus uptake by plants, F_{bcm} (Eq. 18) is biochemical mineralisation, and F_{min} is the ~~net~~ biological mineralization of phosphorus (Parton et al., 1993). The fraction of adsorbed to total soil labile phosphorus is derived from a global dataset of soil phosphorus fractions Yang et al. (2013) and we use USDA soil order specific parameter values. Further, we assume a constant rate at which adsorbed mineral phosphorus becomes strongly sorbed (τ_{sorb}) and is subsequently fixed into secondary minerals. The turnover time of sorbed phosphorus

10   with respect to occlusion is derived from the difference in occluded phosphorus among the sites of the Hawaii chronosequence (Violette in prep.).

2.1.6   Root zone mineral phosphorus

As the mobility of phosphorus in soil is very low, plant uptake tends to be limited by the replenishment of phosphorus to the root surface rather than by the root uptake capacity itself (Schachtman et al., 1998). We simulate the labile phosphorus

15   concentration in soil solution in root contact as a function of plant uptake and diffusion of phosphorus from the surrounding towards the root surface without a vertical discretization. We assume that plant uptake is small compared to the actual amount of dissolved phosphorus in total soil volume (Johnson et al., 2003), and thus its effect on the dissolved phosphorus concentration is limited to a small band around the surface of roots. The diffusion of phosphorus from the surrounding to the root surface (F_{diff}) follows Fick's Law:

20   $$F_{diff} = -D\Delta P_{sol} \tag{22}$$

Where D is the permeability of the soil to phosphorus and ΔP_{sol} is the difference in the phosphorus concentrations between the soil solution at the root surface ($a_{root}\frac{P_{sol}}{\Theta}$) and solution in the surrounding soil volume outside the diffusive zone around the root ($\frac{P_{sol}}{\Theta}$). Assuming a homogeneous distribution of soil water, changes in the phosphorus concentration in the root zone are given by:

25   $$\Delta P_{sol} = (a_{root} - 1)\frac{P_{sol}}{\Theta} \tag{23}$$

where Θ is the volumetric soil water content and a_{root} is the relative reduction of labile phosphorus in soil solution at the root surface compared to the surrounding. As $a_{root} \leq 1$ the diffusion is a single direction flux.

The permeability D is calculated analog to the diffusion coefficient of phosphorus in soils following BARRACLOUGH and TINKER (1981) which accounts for the increased path length in soil using a tortuosity factor (tf). D is further corrected for

half the path length between uniform distributed root cylinders (r_{diff}):

$$D = D_0 c_\Theta \Theta t f \frac{1}{r_{diff}} \qquad (24)$$

Where D_0 is the diffusion coefficient in free water, Θ the volumetric soil water content, and c_Θ a unit conversion factor.

The tortuosity factor is given by a broken-line function of Θ (BARRACLOUGH and TINKER, 1981):

5
$$t f = \begin{cases} f_1 \Theta + f_2 & \text{for } \Theta \geq \Theta_l \\ \frac{\Theta(f_1 \Theta + f_2)}{\Theta_l} & \text{otherwise} \end{cases} \qquad (25)$$

where Θ_l is the soil water content at which the two functions intercept , and f_1 and f_2 are empirical parameters (BARRA-CLOUGH and TINKER, 1981).

We assume that the diffusion path (r_{diff}) can be approximated by half the distance between uniformly distributed roots. We restrict the diffusion path length to $0.1 \, \mathrm{m}$, as the effect of active root phosphorus uptake on the soil phosphorus concentration in

10 distance of more than $10 \, \mathrm{cm}$ is negligible (Li et al., 1991). Following Bonan et al. (2014), we derive half the distance between roots as:

$$r_{diff} = min(0.1, (\pi RLD)^{0.5}) \qquad (26)$$

where the root length density (RLD) (root length per volume of soil) is given by

$$RLD = \frac{M_{root}^*}{r_d \pi r_r^2} \qquad (27)$$

15 where r_d is the root specific density and πr_r^2 is the cross sectional area calculated from fine root radius, r_r, and M_{root}^* the root biomass density in the soil volume.

The ~~changes~~ change in the difference in the dissolved labile phosphorus concentration between the root surface and the surrounding, a_{root}, ~~are~~ is then derived by

$$\frac{da_{root}}{dt} = \frac{F_{diff} - F_{up}}{P_{sol}} \qquad (28)$$

20 Where F_{up} is plant uptake of phosphorus as described earlier.

2.1.7 ~~Biological nitrogen fixation~~

~~While inputs of nitrogen from nitrogen-rich sedimentary rocks can make a significant contribution to the nitrogen budget of specific sites (Holloway, 2002; Morford et al., 2011), the major natural inputs are from biological fixation of atmospheric dinitrogen which is in ample supply (Vitousek et al., 2013). Biological nitrogen fixation (BNF) represents a key process which~~

25 ~~can enhance nitrogen availability under elevated CO$_2$ (Figure ??). Here we use a commonly used representation of BNF which is derived from an empirical correlation between BNF (F_{BNF}) and evapotranspiration (ET) (Cleveland et al., 1999) in which ET is substituted with NPP as they are highly correlated (Thornton et al., 2007): where β_{BNF} is an empirical coefficients~~

2.1.7 Competition between microbes and plants

The competition between microbes and plants for dissolved labile phosphorus is handled analog to the competition for soil mineral nitrogen (Zaehle and Friend, 2010). Gross phosphorus immobilization, gross biological phosphorus mineralization, biochemical mineralization, as well as plant phosphorus uptake are calculated half-hourly. At any time-step, immobilization due to litter and soil organic matter decomposition is given priority in accessing nutrients from gross biological mineralization. This is in line with recent findings regarding the variability in the nitrogen use efficiency of microbes (Mooshammer et al., 2014) which indicates a dominance of microbes in accessing soil nitrogen and results in increasing immobilization with decreasing litter nutrient content(Figure ??).

The nutrient requirement for the built-up of soil organic matter, which affects the nutrients retained from litter decomposition, is dependent on the C:N:P ratio of soil organic matter, whereas the C:N ratios depend on the soil mineral nitrogen concentration (Zaehle and Friend, 2010). Increasing plant uptake of nitrogen reduces the soil mineral nitrogen concentration and thereby reduces the nitrogen retained from litter decomposition in soil organic matter due to its effect on soil C:N ratios.

2.1.8 Input fields

The parameter describing soil phosphorus sorption (k_s) is USDA soil order specific. The parameters for phosphorus release from minerals ($s_{shield}, w_l, E_{a,l}$) are lithological class specific and read in from GliM lithological map (Hartmann and Moosdorf, 2012).

2.2 Site scale simulation

The long-term field fertilization experiment along the Hawaiian soil development chronosequence provides an ideal test case for the nutrient components of ORCHIDEE (Vitousek, 2004). We selected sites for which sufficient observational data are available (Harrington et al., 2001; Ostertag, 2001): a 300 year old site which is nitrogen limited (Thurston) and a 4.1 Million year old site which is phosphorus limited (KokeKokee). The two sites have similar climatic conditions (Table 3) and are dominated by the same tree *Metrosideros polymorpha* (Crews et al., 1995).

We run the model with observed meteorological data (Harris et al., 2014; Thornton et al., 2016) prescribing nutrient boundary conditions, namely inputs of phosphorus and nitrogen by atmospheric deposition (Chadwick et al., 1999) and inputs of phosphorus by weathering (Crews et al., 1995). To do so, we deactivated the module for dynamic phosphorus weathering (see

Table 1. Variables of the model.

Variable	Units	Description
$V_{cmax,h}$	$\mu mol(CO_2)m^{-2}s^{-1}$	maximum carboxylation rate of photosynthesis at canopy level $h; h \in \{1,2,\ldots,20\}$ per leaf area
$J_{max,h}$	$\mu mol(CO_2)m^{-2}s^{-1}$	maximum electron transport capacity of photosynthesis at canopy level $h; h \in \{1,2,\ldots,20\}$ per leaf area
$N_{leaf,h}^*$	$g(N)m^{-2}$	leaf nitrogen concentration at canopy level $h; h \in \{1,2,\ldots,20\}$ per leaf area
u_{max}	$g(P)g^{-1}(C)t^{-1}$	root uptake capacity
C_i	$g(C)m^{-2}$	carbon in plant tissue $i; i \in \{leaf, root, sapwood, heartwood, coarseroot, fruit\}$
a_{root}	–	relative reduction in dissolved phosphorus concentration at root surface
Θ	mm	soil water content
P_{sol}	$g(P)m^{-2}$	dissolved labile phosphorus in soil
P_{sorb}	$g(P)m^{-2}$	adsorbed labile phosphorus in soil
F_{up}	$g(P)m^{-2}t^{-1}$	phosphorus uptake of vegetation
T_{soil}	K	soil temperature
fPN_{plant}	–	scaling function
f_{temp}	–	temperature scaling function of biological activity
pn_{plant}	$g(P)g^{-1}(N)$	phosphorus to nitrogen ratio of active and easily translocatable portion of plant nutrients
P_i	$g(P)m^{-2}$	phosphorus in plant tissue $i; i \in \{leaf, root, sapwood, heartwood, coarseroot, fruit\}$
N_i	$g(N)m^{-2}$	nitrogen in plant tissue $i; i \in \{leaf, root, sapwood, heartwood, coarseroot, fruit\}$
G_P	$g(P)m^{-2}t^{-1}$	phosphorus allocated to growth
$F_{reserve}$	$g(P)m^{-2}t^{-1}$	flux between plant labile and reserve phosphorus pools
$P_{labile,max}$	$g(P)m^{-2}$	maximum size of plant labile phosphorus pool
D_{leaf}	–	empirical elasticity parameter for stoichiometry
pn_{leaf}	$g(P)g^{-1}(N)$	foliage phosphorus to nitrogen ratio
nc_{leaf}	$Pg(N)g^{-1}(C)$	foliage nitrogen to carbon ratio
G_C	$g(C)m^{-2}t^{-1}$	carbon allocated to growth
g_{max}	0.95	daily fraction of P_{labile} available for growth
p_{lim}	–	growth limitation factor derived from phosphorus availability
n_{lim}	–	growth limitation factor derived from nitrogen availability
np_{lim}	–	actual growth limitation factor
$n_{scal,P}$	–	scaling factor for allocation derived from phosphorus availability
$n_{scal,N}$	–	scaling factor for allocation derived from nitrogen availability
n_{scal}	–	actual scaling factor for allocation
pc_{plant}	$g(P)g^{-1}(C)$	growing season average of the plant labile phosphorus to labile carbon concentrations
F_{bcm}	$g(P)m^{-2}t^{-1}$	biochemical mineralization rate of phosphorus
P_x	$g(P)m^{-2}$	phosphorus in soil organic matter $x; x \in \{active, slow, stable\}$
F_{leach}	$g(P)m^{-2}t^{-1}$	dissolved labile phosphorus losses by leaching
F_{weath}	$g(P)m^{-2}t^{-1}$	phosphorus release from primary minerals
F_{min}	$g(P)m^{-2}t^{-1}$	phosphorus release from primary minerals
F_{diff}	$gm^{-2}t^{-1}$	diffusion of phosphorus to the root zone
ΔP_{sol}	$g(P)m^{-3}$	root zone concentration gradient
α_{root}	–	relative reduction of dissolved labile phosphorus in soil solution at the root
D	mt^{-1}	soil permeability to phosphorus
r_{diff}	m	half distance between root cylinders
tf	–	tortuosity factor of diffusion
RLD	mm^{-3}	root length per volume of soil
M_{root}^*	$g(C)m^{-3}$	root biomass density in soil volume

Table 2. Parameter of the model.

Parameter	Value	Units	Description	Source
t	0.0208333	day	time step of 30 minutes	–
nue	PFT specific	$\mu\text{mol(CO}_2)\text{g}^{-1}(\text{N})\text{s}^{-1}$	nitrogen use efficiency of photosynthesis	Kattge et al. (2009)
N_{str}	$4.\times10^{-3}$	$\text{g(N)g}^{-1}(\text{C})$	structural leaf nitrogen	Ali et al. (2015)
κ_N	0.11	m^2m^{-2}	canopy nitrogen extinction coefficient	Zaehle and Friend (2010)
v_{max}	4.31×10^{-6}	$\text{g(P)}\,\text{g(C)}\,\text{t}^{-1}$	maximal uptake capacity of roots	calibrated
K_{Pmin}	3.	$\mu\text{mol(P)l}^{-1}$	dissolved phosphorus concentration at which uptake equals $\frac{v_{max}}{2}$	Schachtman et al. (1998)
k_{Pmin}	0.01	$\mu\text{mol(P)l}^{-1}$	linear increase in p uptake for high phosphorus concentrations	calibrated Zhang et al. (2009)
c_k	depends on soil order	lg(P)^{-1}	unit conversion factor	this study
$T_{soil,ref}$	303.15	K	reference soil temperature	(Zaehle and Friend, 2010)
$pn_{leaf,min}$	PFT specific	$\text{g(P)g}^{-1}(\text{N})$	minimum foliage phosphorus to nitrogen ratio	McGroddy et al. (2004)
$pn_{leaf,max}$	PFT specific	$\text{g(P)g}^{-1}(\text{N})$	maximum foliage phosphorus to nitrogen ratio	McGroddy et al. (2004)
$nc_{leaf,min}$	PFT specific	$\text{Pg(N)g}^{-1}(\text{C})$	minimum foliage nitrogen to carbon ratio	Zaehle and Friend (2010)
$nc_{leaf,max}$	PFT specific	$\text{Pg(N)g}^{-1}(\text{C})$	maximum foliage nitrogen to carbon ratio	Zaehle and Friend (2010)
$pc_{leaf,ave}$	PFT specific	$\text{g(P)g}^{-1}(\text{C})$	average leaf phosphorus to carbon ratio	Zaehle and Friend (2010); McGroddy et al. (2004)
τ_i	PFT specific	–	fraction of tissue i shed per time step	Krinner et al. (2005)
$f_{trans,i}$	0.57	–	retranslocated fraction of tissue phosphorus	McGroddy et al. (2004)
λ_i	PFT and tissue specific	$\text{g(P)g}^{-1}(\text{C})$	phosphorus to carbon allocation to tissue $i; i \in \{root, sapwood\}$ relative to leaves	McGroddy et al. (2004); Sardans et al. (2015)
D_{max}	0.25	–	maximum change in phosphorus to nitrogen ratio of new biomass	Zaehle and Friend (2010)
			relative to existing biomass	Vuichard in prep.
$\tau_{active,ref}$	3.65	yr^{-1}	inverse of decomposition rate of phosphorus in	
			active soil organic matter pool due to biochemical mineralization	calibrated
$\tau_{slow,ref}$	0.067	yr^{-1}	inverse of decomposition rate of phosphorus in	
			slow soil organic matter pool due to biochemical mineralization	calibrated
$\tau_{passive,ref}$	0.0	yr^{-1}	inverse of decomposition rate of phosphorus in	
			passive soil organic matter pool due to biochemical mineralization	calibrated
k_s	depends on soil order	–	fraction of labile phosphorus adsorbed	Yang and Post (2011)
τ_{sorb}	9125.	day^{-1}	rate of strong sorption	this study
D_0	1.581×10^{-2}	m^2t^{-1}	phosphorus diffusion coefficient in free water at 25 degree C	Mollier et al. (2008)
c_Θ	$1.\times10^{-3}$	–	unit conversion factor	this study
Θ_l	0.12	$\text{m}^3(\text{H}_2\text{O})\text{m}^{-3}(\text{soil})$	soil water content at which the two functions intercept	BARRACLOUGH and TINKER (1981)
f_1	1.58	–	empirical factor	BARRACLOUGH and TINKER (1981)
f_2	-0.17	–	empirical factor	BARRACLOUGH and TINKER (1981)
r_d	0.15×10^6	$\text{g(C)m}^{-3}(\text{root})$	root specific density	Bonan et al. (2014)
r_r	0.29×10^{-3}	m	root radius	Bonan et al. (2014)

appendix) and instead prescribed a constant site-specific release rate. In addition, we prescribe site specific physico-chemical soil properties (Crews et al., 1995; Chorover et al., 2004; Olander and Vitousek, 2004). The prescribed vegetation cover is tropical evergreen broadleaf vegetation.

We equilibrated the biogeochemical cycles of the 4.1 million yr old site to the climatic conditions and the nutrient inputs using the semi-analytical spinup procedure (Naudts et al., 2015) which was extended to handle nutrient cycles. To capture the transitional nature of the 300 yr old site, we perform a 230 year long spinup simulation. The differences between the simulation duration and the actual age of the site is due to a correction for an initial amount of biomass we have to set in ORCHIDEE due to technical reason (see appendix C).

We extended the spinup simulations of both sites into a set of three nutrient addition simulations: adding only nitrogen, only phosphorus, and nitrogen and phosphorus together. A total of $10\,\text{g(N)m}^{-2}\text{yr}^{-1}$ and $10\,\text{g(P)m}^{-2}\text{yr}^{-1}$ are added in the model

simulations homogeneously distributed across the year. In the field the same amount per year was applied, but semi-annually (Harrington et al., 2001; Ostertag, 2001).

2.2.1 Forcing data

The meteorological forcing data for ORCHIDEE is derived from Daily Surface Weather Data on a 1-km Grid for North America (DAYMET), Version 3 (Thornton et al., 2016). The data includes meteorological information (short-wave radiation, maximum daily temperature, minimum daily temperature, daily precipitation sum) for the period 1980–2013. In DAYMET, the mean annual surface temperature and annual sum of precipitation for the actual locations of the two sites (Table 3) substantially deviate from the values reported at site (Crews et al., 1995). Therefore, we pick the closest site nearby Thurston (16km distance; lat=19.8318,lon= -155.411) which has an annual sum of precipitation of 2500 ± 250 mmyr^{-1} and an average annual temperature 16 ± 1 °C as reported in Crews et al. (1995) and use it for both sites (as the DAYMET data for the ~~Koke~~ Kokee island did not include any grid point with appropriate climate).

We extract additional information which is needed to run ORCHIDEE, namely surface pressure, long-wave downward radiation, and wind, from a 0.5 x 0.5 degree reanalysis data set (CRU-NCEP) (Harris et al., 2014) using the coordinates of the Thurston site. We correct surface pressure from CRU-NCEP with the actual altitude of each site using a lapse rate and derive specific humidity from water pressure, air temperature and surface pressure.

The annual inputs of nutrients by atmospheric deposition and weathering (Table 3) are kept constant and are evenly distributed throughout the year.

2.2.2 Site specific parametrization

We use site information collected from literature (Harrington et al., 2001; Ostertag, 2001) to parametrize the model (Table 3). We account for differences in the soil characteristics between sites, but use a ~~a~~ common parametrization for all biological processes. Thereby, we are able to evaluate the differences in vegetation due to differences in soil characteristics and chemical weathering solely.

As soils are not vertically discretized in ORCHIDEE, we average observations when given for different soil horizons. The soil fractions for the Thurston are assumed to be 50% sand and 25% silt and 25% clay due to lack of site specific information.

We ~~calibrate the soil phosphorus sorption coefficient, k_s, of the 4.1site by adjusting phosphorus availability so that simulated net primary productivity is close to observations. The value of k_s for~~ account for changes in the sorption characteristics of volcanic soils are they develop. For the 300yr site~~is derived from the calibrated value for~~, we use the average value of k_s for Andisols from (Yang and Post, 2011). For the 4.1~~k yr site and~~Myr site k_s was scaled with the relative difference in soil phosphorus sorption capacity between the two sites as computed dynamically in the P-enabled version (Violette in prep) of the mechanistic weathering model WITCH (Goddéris et al., 2006). P release rates from primary and secondary minerals are inferred from the observed differences in the chemical composition of minerals between sites along the chronosequence from (Crews et al., 1995) (Violette in prep).

The reference decomposition rate of soil organic matter pools by biochemical mineralization ($\tau_{x,ref}$) are chosen so that the nitrogen to phosphorus ratio of soil organic matter is close to observation of approximately 10 g(N)g^{-1}((P) for sites older than 10kyr in the Hawaiian chronosequence (Crews et al., 1995). This is a common procedure Wang et al. (2010); Goll et al. (2012); Yang et al. (2014) as this flux remains yet to be quantified in the field.

5　　We prescribe observed values for specific leaf area, which is a fixed parameter and does not vary over time, and use the 25th and 75th percentile of observed values of leaf P:N of the dominant tree species (KATTGE et al., 2011) as boundaries for the leaf P:N ratio. We further increase the critical leaf age, which scales leaf turnover related to leaf age in ORCHIDEE, from 1.4 yr to 6 yr to account for the substantially longer lifespan of leaves at both sites (Harrington et al., 2001) compared to the default value of ORCHIDEE (Naudts et al., 2015).

10　　Following Yang et al. (2014), we adjust the turnover of the passive soil organic matter pools to achieve soil organic carbon stocks at the 4.1close to the observations. The adjusted parameters same turnover rates are used for both sites.

　　The remaining parameter (including parameter for biological nitrogen fixation) are taken from the global parametrization of ORCHIDEE of the tropical evergreen broadleaf PFT (SI Table A1).

2.2.3　Analysis

15　We aggregate estimates of root production approximated by soil respiration from Ostertag (2001) and compare it to the simulated below-ground component of NPP (namely, NPP allocated to below-ground sapwood, below-ground heartwood, and fine roots). We sum the simulated above-ground component of NPP allocated to sapwood and heartwood and compare it to estimates of wood production based on wood increment and woody litter fall (Harrington et al., 2001). All other components of simulated NPP (fruit, leaf, reserve) are pooled and compared to estimates of non-woody NPP based on litterfall (Harrington

20　et al., 2001). Simulated nutrient use efficiencies (NUE,PUE) are calculated as

$$XUE = \frac{NPP}{X_{uptake}} \tag{29}$$

where NPP is annual NPP and X_{uptake} the annual uptake of nutrient $X; X \in \{N, P\}$. Simulated nutrient use efficiencies are then compared to estimates derived from on leaf litter fall, root growth and wood increment in combination with the chemical composition of leaves and wood (Harrington et al., 2001). We further separated the nutrient use efficiencies into its underlying

25　components, carbon production rate per biomass nutrient (X_{prod}) and nutrient residence time (X_{MRT}), following Finzi et al. (2007):

$$XUE = \underbrace{\frac{NPP}{X_{content}}}_{X_{prod}} \times \underbrace{\frac{X_{content}}{X_{uptake}}}_{X_{MRT}} \tag{30}$$

where $X_{content}$ is the whole plant content [g(X)m^{-2}] of nutrient $X; X \in \{N, P\}$. No information on below-ground productivity is available for the fertilization treatment (Harrington et al., 2001). Thus, we calculate above-ground nutrient use efficiencies

30　($aNUE$,$aPNUE$) using above-ground NPP instead of total NPP.

Table 3. The site conditions prescribed for the simulation for the 300yr old site and the 4.1Myr old site along the Hawaii chronosequence.

	Thurston	~~Koke~~ Kokee	Source
latitude [$^\circ$N]	19.4140	22.1390	Vitousek (2004)
longitude [$^\circ$W]	155.2353	159.6245	Vitousek (2004)
altitude [m]	1176	1134	Crews et al. (1995)
age [yr]	300	4.1×10^6	Vitousek (2004)
mean annual temperature [$^\circ$C]	16	16	Crews et al. (1995)
mean annual precipitation [$\mathrm{mm\,yr^{-1}}$]	2500	2500	Crews et al. (1995)
N deposition [$\mathrm{g\,m^{-2}\,yr^{-1}}$]	0.6±0.4	0.6±0.4	Chadwick et al. (1999)
P deposition [$\mathrm{mg\,m^{-2}\,yr^{-1}}$]	0.9±0.3	0.9±0.3	Chadwick et al. (1999)
P release [$\mathrm{mg\,m^{-2}\,yr^{-1}}$]	434.0	0.265	Violette in prep.
soil order	Entisols	Oxisols	Vitousek (2004)
soil pH	5.0	3.8	Chorover et al. (2004)
soil bulk density [$\mathrm{kg\,m^{-2}}$]	300	575	Olander and Vitousek (2004)
soil texture (clay:silt:sand) [%]	25:25:50	17:79:4	Olander and Vitousek (2004)
dissolved fraction labile P ($1\text{-}k_s$) [ ]	~~140×10^{-3}~~ 0.4	~~70×10^{-3}~~ 0.2	Violette in prep.
specific leaf area [$\mathrm{m^2 g^{-1}}$(C)]	11.236×10^{-3}	11.236×10^{-3}	Vitousek (2004)
max. foliage N:P ratio ($np_{leaf,max}$)[g(N)g^{-1}(P)]	18.	18.	(Kattge et al., 2009)
min. foliage N:P ratio ($np_{leaf,min}$)[g(N)g^{-1}(P)]	12.83	12.83	(Kattge et al., 2009)
critical leaf age [yr]	5.9	5.9	Harrington et al. (2001)

Simulated apparent leaf lifespan (including climatic effects) is calculated by dividing the annual mean of leaf mass by the annual sum of NPP allocated to leaf growth. We calculate the rate by which soil organic phosphorus is biochemically mineralized and compare it to measurements of phosphatase activity (Olander and Vitousek, 2000) as a proxy of potential biochemical mineralization due to lack of alternatives.

The uncertainty ranges of simulated variables are given by the standard deviation of annual values. We perform Student's t-tests to determine if the fertilization treatments resulted in significantly differences in the tested variables compared to the control experiment in observations (when sufficient information is available) and simulations.

3 Results & discussion

3.1 Control simulation

The comparison of carbon and nutrient cycle related ecosystem properties in the control simulations with observations allow to detect model biases which facilitate the evaluation of the outcome of the fertilization experiments.

Table 4. Vegetation characteristics at the 300yr old site and the 4.1Myr old site along the Hawaii chronosequence under natural nutrient condition (control simulation) (mean±standard deviation). The observation based estimates (mean±standard deviation) are from Crews et al. (2001); Harrington et al. (2001); Ostertag (2001). * prescribed parameter. # from a nearby side. Standard deviation of observation only given when sufficient information is available in the original publication.

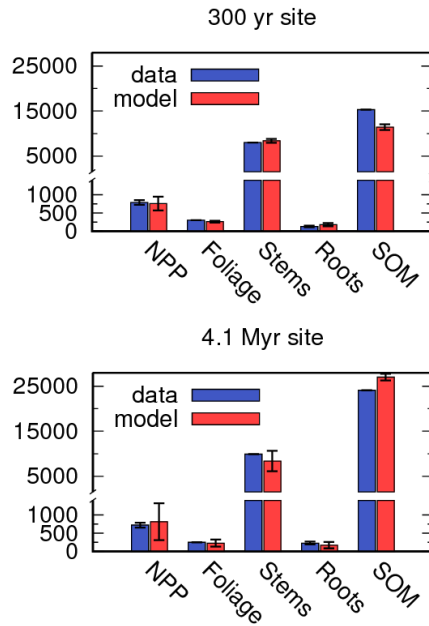|	300yr old site		4.1Myr old site	
	simulated	observed	simulated	observed
NPP [$gm^{-2}yr^{-1}$]	~~784.~~758.±347.	789.±63.	~~710.±575.~~816.±503.	757±73
NPP$_{leaf}$[%]	~~16.~~17.	25.	~~15.~~14.	21.
NPP$_{stem}$[%]	60.	41.	~~62.~~65.	50.
NPP$_{root}$[%]	~~24.~~23.	34.	~~23.~~21.	28.
NUE [$g(C)g^{-1}(N)$]	~~115.91~~165.7±303.5	229.9±17.9	~~103.0~~115.8±89.7	224.8±32.7
N_{up}[$g(N)m^{-2}yr^{-1}$]	4.53±1.97	3.43	7.04±5.46	3.21
N_{plant} [$g(N)m^{-2}$]	39.1±1.95	28.8#	70.1±15.1	28.8#
N_{prod} [$g(C)g^{-1}(N)yr^{-1}$]	~~12.1±5.4~~19.2±4.8	27.3	~~12.2±7.8~~11.6±6.6	25.0
N_{MRT} [yr]	~~9.5±112.2~~8.6±94.6	8.4	~~8.4±19.9~~9.96±195.77	9.0
PUE [$g(C)mg^{-1}(P)$]	~~1.63±6.04~~2.67±0.61	3.22±0.23	~~1.85±1.07~~1.89±2.53	3.86±0.53
P_{up} [$g(P)m^{-2}yr^{-1}$]	0.30±0.10	0.24	0.43±0.32	0.19
P_{plant} [$g(P)m^{-2}$]	2.60±0.08	2.99#	3.2±1.4	2.99#
P_{prod} [$g(C)mg^{-1}(P)yr^{-1}$]	~~0.17±0.08~~0.29±0.07	0.26	~~0.28±0.21~~0.27±0.16	0.24
P_{MRT} [yr]	~~9.6±162.2~~9.3±4.3	12.2	~~7.3±60.5~~7.4±54.9	16.0
biological nitrogen fixation [$g(N)yr^{-1}$]	~~2.25±.96~~2.20±.48	2–3	~~1.71±.32~~1.16±1.42	–
leaf lifespan [yr]	~~7.6~~8.2±5.3	8.2±1.8	~~6.3±4.5~~7.7±10.1	3.6±0.6
leaf nitrogen content [% (dry weight)]	~~1.33±0.10~~0.93±0.04	0.73±0.05	~~1.19±0.41~~1.12±0.30	0.95±0.13
leaf phosphorus content [‰(dry weight)]	~~0.88±0.11~~0.61±1.99	0.58±0.06	~~0.66±0.00~~0.64±0.03	0.55±0.04
leaf N:P ratio [$g(N)g^{-1}(P)$]	~~15.1±1.6~~15.2±1.1	12.6±1.6	~~18.0~~17.5±0.03	17.3±2.7
N retranslocated [%]	50*	41±12	50*	55±6
P retranslocated [%]	57*	50±9	57*	59±3
labile P concentration [$mg(P)m^{-2}$]	3.0±3.3	–	1.17±0.88	–
mineral N concentration [$g(N)m^{-2}$]	0.04±0.02	–	1.79±1.42	–

18

Figure 3. Comparison between simulations (mean±standard deviation) and observations (mean±standard deviation - if available) at the 300yr old site (a), and the 4.1Myr old site (b) along the Hawaii chronosequence. Net primary productivity (NPP) is given in $g(C)m^{-2}yr^{-1}$, the standing stocks of foliage, stems (incl. coarse roots), fine roots, and soil organic matter (SOM) are given in $g(C)m^{-2}$. The standard deviation in case of simulations indicates the inter-annual variability, not model error.

Net primary productivity (NPP) at both sites is well reproduced by the model (Figure 3). ~~The good agreement of NPP at the 4.1site is due to the calibration of the dissolved fraction labile phosphorus (k_s). The NPP at the 300~~At both site was not calibrated and thus is an independent model outcome. The simulated inter-annual variation in NPP at the 4.1Myr site is ~~very large compared to~~ more than twice as large as at the 300yr site. ~~The larger variability is caused by an amplification of~~

5 ~~the drought induced reduction in plant growth under conditions of low phosphorus availability: During periods of drought the soil permeability to phosphorus is reduced and the root zone is more likely to get phosphorus depleted (see appendix ??). During longer periods of drought the increased litterfall and subsequent immobilization of phosphorus during litter decomposition further reduces the overall soil phosphorus availability. As a result plant access to phosphorus is lowered and growth diminished.~~ The model tends to capture the allocation pattern of NPP to the different plant tissues (Table 4). While

10 wood growth is overestimated at both sites, the relative allocation to leaf and roots is rather well reproduced: The simulated ratio between root and leaf growth of ~~1.50 and 1.53~~ 1.35 and 1.50 for the 300yr and 4.1Myr site, respectively, is ~~somewhat higher than observed (~~are close to the observed ratios of 1.36 and 1.33~~)~~. This shows that the allocation scheme in ORCHIDEE, which accounts in a simplistic way for changes in the allocated fraction of NPP into below-ground allocation in response to stress (light, nutrient, water) (Zaehle and Friend, 2010; Naudts et al., 2015) gives reasonable results.

15 The simulated biomass stocks are in good agreement with the observations, with the exception of ~~fine root mass at the 300site and~~ woody biomass at the 4.1Myr site (Figure 3). As wood growth is overestimated, the low woody biomass can be linked to

19

an overestimation of wood turnover (appendix D). Comparably, the slight overestimation of fine root biomass at the 300yr site is linked to a too high turnover of fine roots (appendix D). The large differences in observed fine root turnover between sites (Ostertag, 2001) cannot be captured by the model as fine root turnover is constant in ORCHIDEE.

Nutrient use efficiencies (NPP divided by plant nutrient uptake) are implicit plant properties that depend on the tissue stoichiometry, as well as the relative allocation of NPP to the various plant organs and their respective turnover rates. The nitrogen use efficiency (NUE) and phosphorus use efficiency (PUE) are underestimated between 50–60% at both sites 20–50% (Table 4). The analysis of the underlying components of nutrient use efficiencies following Finzi et al. (2007) (Equation 30), indicate that the underestimation of NUE is mainly driven by the low carbon productivity per plant nitrogen (N_{prod}), while the low bias in PUE is due to a combination of low P_{prod} and the short residence time of plant phosphorus (P_{MRT}) (appendix D). The low N_{prod} and P_{prod} at the 300yr site can be attributed to the overestimation wood biomass and its nitrogen content (appendix D). At the 4.1yr site the underestimation of nutrient content of biomass and wood biomass has opposing effects on the nutrient use efficiencies. The general underestimation of the residence time of phosphorus (Table 4) is likely due a underestimation of the phosphorus content of long-lived plant tissue and the overestimation of wood turnover. Additionally, the extremely low concentration of plant available phosphorus at the 4.1Myr site results in a set of physiological and morphological adaptations mechanisms which increase P_{MRT} but are not resolved in ORCHIDEE (for example changes in root morphology and turnover and leaf phosphorus recycling) (Schachtman et al., 1998; Niu et al., 2013; Reed et al., 2015). In ORCHIDEE the somewhat longer nutrient residences times at the young site are primarily due to the site's transient state in which biomass is still accumulating (appendix D).

The simulated inter-annual variabilities in nutrient use efficiencies, in particular in the simulated NUE at the 300yr site, are very large due a substantial, but highly variable, contribution of nutrients from internal reserves to new biomass growth (not shown). Reserves can amount of up to 75% of peak nutrient content in fine roots and leaves during the last growing season for evergreen plant functional types in ORCHIDEE (Zaehle and Friend, 2010). In the model, variations in reserves can be large in nutrient poor environments which are subject to periods of reduced growth unrelated to nutrient starvation (here: drought). During droughts the nitrogen reserves are filled with foliage nitrogen which is recycled prior leaf fall, while the nitrogen reserves are depleted when water availability and subsequent growth is high. Defoliation experiments indicate that plants can rely on substantial amounts of internally stored reserves of carbohydrate and nutrients which allow them to survive multiple defoliation events (Hartmann and Trumbore, 2016), however the extent to which plant rely on internal storages are strongly species dependent (Piper and Fajardo, 2014), and the role of nutrient is often overlooked (Hartmann and Trumbore, 2016). Nonetheless, Ichie and Nakagawa (2013) showed that in *Dryobalanops aromatica* stored phosphorus accounted for 67.7% of the total phosphorus requirements for reproduction, while stored N accounted for only 19.7%, indicating substantial nutrient reserves in tropical trees.

The simulated leaf N:P ratio is with 15.1 15.2 at the 300yr site somewhat higher than the observation of 12.6±1.56, which lies just outside the lower boundary ($np_{leaf,min}$) of 12.83 in ORCHIDEE (Table 4). At the 4.1Myr site, the simulated leaf N:P ratio is with 18.0 17.5 g(N)g^{-1}(P) very close to the observation of 17.3 g(N)g^{-1}(P) and equals the upper boundary prescribed in ORCHIDEE ($np_{leaf,max}$). Foliage N:P ratios of less than 14 are commonly associated with nitrogen limitation and ratios

above 16 with phosphorus limitation (Koerselman and Meuleman, 1996). Although simulated leaf nitrogen concentration of ~~1.19~~ 0.93 %(dryweight) ~~is 60~~at the 300yr site, is 27% higher than observed, it is substantially lower than the optimal concentration prescribed ($cn_{leaf,min}$) of 3.33 %dryweight) indicating substantial effects of ~~nitrogen stress~~ the low soil nitrogen concentration (Table 4) on productivity and allocation at the 300 yr site in the model. Thus, despite being useful tools, the common use of threshold stoichiometric ratios and models with rigid plant traits is somewhat limited when it comes to species specific responses (Verheijen et al., 2016).

The differences in stoichiometry mirror differences in the respective availabilities of mineral nitrogen and soil labile phosphorus (Table 4) . While the concentration of mineral nitrogen is extremely low at the young site due to a high immobilization demand of accumulating soil organic matter, the concentration is high at the old site where immobilization demand is met by the mineralisation of nitrogen from organic matter. In case of phosphorus, the high phosphorus input of 434. $\mathrm{mgm^{-2}yr^{-1}}$ at the 300yr site keep soil labile phosphorus concentration high despite the high immobilization demand. At the the old site, the extremely low phosphorus inputs of 0.27 $\mathrm{mgm^{-2}yr^{-1}}$ result in low soil labile phosphorus concentration as the ecosystem relies primarily on the mineralisation of phosphorus from soil organic matter.

At the 300yr site, the simulated C:N:P stoichiometry of soil organic matter is with 309:16:1 nearly twice as rich in phosphorus as observed (425:28:1). As no significant difference in phosphatases activities among sites were observed (Ostertag, 2001) and the biochemical mineralization in ORCHIDEE is calibrated to achieve realistic phosphorus concentration in soil organic matter on the long term (4.1Myr site), the deviation of the simulated from observed phosphorus concentrations has to processes other than biochemical mineralization. A recent data analysis suggests that during initial stages of decomposition losses of carbon and phosphorus are proportional, but there are smaller relative losses of nitrogen, due interactions between soil organic matter and the physical soil environment (Tipping et al., 2016). Reduced losses of nitrogen during initial stages of decomposition would lead to elevated N:P during early stages of soil development compared to later stages. As the simplistic soil decomposition in ORCHIDEE (Parton et al., 1993) omits interactions between soil organic matter and the physical soil environment (Doetterl et al., 2015; Tipping et al., 2016), it fails to reproduce the strong influence of litter stoichiometry on the overall soil stoichiometry.

At the 4.1Myr site, the C:N:P stoichiometry of the soil organic matter is with 158:12:1 relatively close to the observed C:N:P ratio of 215:10:1. The realistic phosphorus content of soil organic matter indicates that the relative contribution of biochemical mineralization is sufficiently well calibrated in the model. It has to be noted, that recent findings indicate a preferential physical stabilization of nutrient rich soil organic matter (Tipping et al., 2016) and a role of phosphatases in rendering organic compounds available as a carbon source to microbes (Spohn and Kuzyakov, 2013). Both findings challenge the classical view of a primary control of biochemical mineralization on the soil organic matter phosphorus concentration (Walker and Syers, 1976). Thus the common calibration approach (Wang et al., 2010; Goll et al., 2012; Yang et al., 2014) might be shortsighted.

The nitrogen fixation rate of 2.25±.96 $\mathrm{gm^{-2}}$ at the 300yr site lies within the range observed among sites during early (<150yr) soil development in Hawaii (Crews et al., 2001) (Table 4). The lower fixation rates at the 4.1Myr site ~~indicate a higher availability of nitrogen from the soil than at the 300site~~is due to the high mineral nitrogen availability. As the regulation mechanisms of nitrogen fixation are elusive (Barron et al., 2009; Vitousek et al., 2013) we only account for direct product inhi-

bition control, a common regulation mechanism in biological systems, via soil mineral nitrogen concentrations (Equation B2), omitting a direct influence of phosphorus availability on nitrogen fixation (Vitousek et al., 2013).

In summary, the model is able to capture biomass stocks and NPP ~~reasonably~~ well and - more important - captures the contrasting nutritional states of vegetation among the two sites, indicated by the foliage N:P ratio. As we prescribe a common parametrization of vegetation characteristics for both sites, the differences in the leaf stoichiometry is the emergent outcome of the process governing the access of plants to nutrients and their response to two contrasting situation of nutrient availability ~~.~~ which originate solely from differences in phosphorus inputs, labile phosphorus sorption capacity and organic matter accumulation rate.

The model fails to reproduce difference in the allocation of NPP to different tissue and tissue turnover between sites, due to ~~omission of plasticity in general for~~ insufficient plasticity in tissue turnover and ~~due to insufficient flexibility in processes which account for environmental effects (allocation)~~biomass allocation. The simulations suggest that the recycling and storage of nutrients in ecosystems subject to periods of drought or other nutrient-unrelated declines in foliage and growth are an important source of nutrients for new growth. We show that the approach of calibrating biochemical mineralization rates using the soil organic matter stoichiometry is problematic, which is in line with growing evidence about the physical stabilization of soil organic matter (Doetterl et al., 2015; Tipping et al., 2016) and new insights into the functioning of phosphatase (Spohn and Kuzyakov, 2013). We further show, that despite ORCHIDEE's intended application when designed, the model is able to capture to a large degree the general state of an ecosystem in a early stage of soil development.

3.2 Fertilization experiment

To evaluate the simulated response of vegetation to nutrient addition, we perform three nutrient treatment simulation per site: addition of either nitrogen (+N) or phosphorus (+P), or the combined addition of both (+NP). The annual addition rates of nitrogen and phosphorus of $10 \, \mathrm{g m^{-2} yr^{-1}}$ are similar to the field experiments.

The model captures the signs of change in net primary productivity (NPP) to the fertilization treatments at both sites: at the 300yr site NPP strongly reacts to the addition of nitrogen, but not to the addition of phosphorus, while at the 4.1Myr site NPP strongly reacts to the addition of phosphorus, but not to the addition of nitrogen (Figure 4). For the 4.1Myr site, also the size of the simulated response ratio (defined as NPP of the nutrient addition experiment divided by the NPP of the control experiment) is comparable to the observed response ratio. At the 300yr site, the simulated positive effect of nitrogen deviates from the observation but is still within the range of uncertainty. However, the synergistic effects of combined addition are not captured by the model, as the model simulates a background phosphorus availability at the 300yr site which is high enough to support the nitrogen stimulated growth.

The 300yr site is accumulating organic material, in particular soil organic matter, and the accompanied immobilization of soil nutrients is the major driver of nutrient scarcity. This leads to extremely low mineral nitrogen concentration. whereas the high weathering release of phosphorus from minerals is sufficient to keep soil labile phosphorus concentration relatively high (Table 4). Therefore, vegetation reacts strongly to the addition of nitrogen at the young site. The lack of any stimulation of plant productivity in the model to phosphorus addition at the young site indicates an overestimation of plant available phosphorus
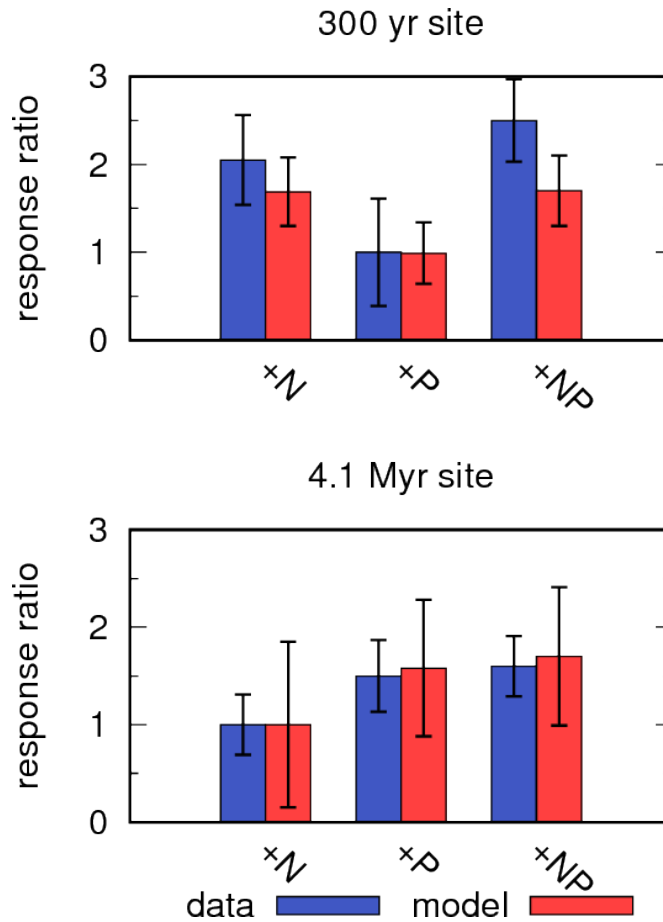
Figure 4. Comparison of simulated and the observed responses of net primary production to fertilization at the 300yr old site (a) and the 4.1Myr old site (b) along the Hawaii chronosequence. The response ratio is the measured or modeled plant production in the fertilizer treatment divided by its value under unfertilized conditions. The bars represent the measurement uncertainty and the annual variability in simulations, respectively.

likely due to the omission of differences in the occlusion rate of soil labile phosphorus among sites which tends to be much higher at the young site (Violette in prep). At the 4.1Myr site the remobilization of phosphorus from soil organic matter is the major source of phosphorus for vegetation, as the minerals are phosphorus depleted leading to low soil labile phosphorus concentration (Table 4). Compared to the young site, also a higher fraction of soil labile phosphorus is adsorbed to soil particles and thus not available to plants. Therefore, vegetation reacts strongly to the addition of phosphorus at the old site, but not to nitrogen addition.

The increases in the NPP per leaf area (NPP/LA) are more pronounced than the increases in leaf area index when nitrogen stress is alleviated (300 yr site), whereas the increases in NPP/LA are comparable to the increases in leaf area index when phosphorus stress is alleviated (4.1 Myr site) (Table 5), in both model and observations. Such a model behavior can be expected

Table 5. The response of net primary productivity, leaf area index, nutrient use efficiencies and foliar stoichiometry to nutrient addition at the 300yr old sites and the 4.1Myr old site along the Hawaii chronosequence. Given are the relative difference between the nutrient addition experiments and the control simulation and in brackets in the observed changes (Harrington et al., 2001; Ostertag, 2001). We used a Students t-test to test if nutrient addition resulted in a significant difference in the respective variables. If significant (p>~~0.1~~0.05) the values are in bold.

	300yr old site			4.1Myr old site		
	+N	+P	+NP	+N	+P	+NP
NPP	+~~61~~**69** (+105)%	0 (0)%	+~~60~~**70** (+150)%	-~~4~~0 (0)%	+~~44~~**58** (+50)%	+~~81~~**70** (+60)%
NPP/LA	**+44 (+86)%**	0 (+72)%	+~~43~~**44 (+128)%**	-~~6~~**-2 (+41)%**	+~~7~~-27 (+32)%	**+39 (+31)%**
LAI	**+14** (0)%	0 (-13)%	+~~13~~**14 (+30)%**	+~~5~~-2 (-11)%	+~~40~~**26** (+19)%	+~~38~~**18** (+31)%
ANUE (ANPP/NUP)	-~~22~~**-38** (+11)%	0 (+32)%	-~~21~~**-38** (+12)%	-25 **(-10)%**	+~~3~~-13 (+30)%	-~~23~~**-46 (-20)%**
APUE (ANPP/PUP)	-~~56~~**-35** (+33)%	-~~4~~**-6 (-45)%**	-~~59~~**-41 (-35)%**	+~~27~~0 (+2)%	-~~8~~**-13 (-63)%**	-~~32~~**-68 (-65)%**
foliar N:P ratio	-~~13~~**+3 (+25)%**	-~~4~~**-7 (-45)%**	-~~15~~**-9** (-20)%	0 (-10)%	-~~28~~**-23 (-82)%**	-~~4~~**-23 (-64)%**
foliar N content	+~~40~~**55 (+16)%**	0 (-10)%	+~~46~~**55** (+7)%	-~~15~~**+4 (+11)%**	+~~30~~**38 (-14)%**	+~~106~~**122** (+22)%
foliar P content	+~~61~~**51 (-7)%**	+~~2~~**8 (+64)%**	+70 (+33)%	-~~15~~**+4** (+22)%	+~~66~~**88 (+467)%**	+~~115~~**187 (+342)%**
biochemical mineralization	+~~233~~**92 (+62)%**	-~~21~~**-52 (-63)%**	+~~10~~49 (-23)%	+~~39~~22 (+32)%	-~~67~~**-91 (-24)%**	-~~30~~**-90 (-55)%**

due to lack of a direct effect of foliage phosphorus concentration on photosynthesis (Figure 2). While the link between leaf nitrogen concentration and the carboxylation efficiency of photosynthesis (V_{cmax}) is well established (Kattge et al., 2009), the role of leaf phosphorus concentration on photosynthesis is less clear as nitrogen and phosphorus concentrations usually co-vary (Reich et al., 2009; Kattge et al., 2009; Domingues et al., 2010; Walker et al., 2014; Bahar et al., 2016; Norby et al., 2016).

5   The model fails to capture the drop in leaf area index when the non-limiting nutrient is added (which is phosphorus for the 300yr site and nitrogen for the 4.1Myr site). The causes for the drop are unclear (Harrington et al., 2001), but could be related to a increase in grazing in the fertilized plots due to the higher nutrient content of foliage compared to the surrounding (Casotti and Bradley, 1991; Campo and Dirzo, 2003).

    The model fails to capture the ~~observed reduction in the nutrient use efficiency (NUE, PUE) when~~ the ~~non-limiting nutrient~~ 10 ~~is added(which is phosphorus for the 300site and nitrogen for the 4.1site)~~extent to which phosphorus use efficiency declines when phosphorus is added. This can be attributed to the omission of excessive plant uptake of nutrients (luxury consumption) which drives the observed reduction in the use efficiencies of the non-limiting nutrient (Harrington et al., 2001). As luxury consumption doesn't directly affect plant growth (Lawrence, 2001; Van Wijk et al., 2003) and is strongly species dependent (Lawrence, 2001) it is omitted in the model.

15   The model tends to overestimate increases in leaf nitrogen concentration in response to nitrogen addition, while increases in leaf phosphorus concentration in response to phosphorus addition are underestimated (Table 5). ~~This points towards biases~~ Biases in the availability of added nutrients to vegetation could be responsible for mismatch between observed and simulated responses. ORCHIDEE is prone to overestimate sorption losses when soil labile phosphorus concentration is substantially

elevated above natural levels as the linear phosphorus sorption applied here cannot capture the increase in the dissolved fraction when the sorbed fraction approaches the maximum sorption capacity of the soil. The simulation setup of applying fertilizer evenly during the year instead in two fertilization events, underestimates nitrogen losses due to the non-linear relationship between soil emissions and substrate availability (Shcherbak et al., 2014). However, the stoichiometric adjustments in

5   ORCHIDEE are not process-based and might be itself the cause for the bias in the simulated response of leaf stoichiometry.

The sign of the responses of biochemical mineralization to nutrient addition ~~tend, with some exceptions, to mirror~~ mirrors the observed changes in potential phosphatase activity (Table 5). This indicates that the simplistic approach for biochemical mineralization applied in ORCHIDEE seems to capture the general behavior of phosphatase activity. However, it does not allow do draw any conclusion about the overall significance of biochemical mineralization to total mineralization, which represents

10   a major uncertainty for modeling phosphorus cycling (Goll et al., 2012; Yang et al., 2014; Reed et al., 2015).

In summary, the model is able to capture the contrasting responses to the three fertilization treatments among the two sites. We find further that differences between sites in the underlying changes in LAI and NPP/LA are partly captured by the model: The alleviation of nitrogen stress at the 300yr site increases NPP/LA more strongly than LAI, while the alleviation of phosphorus stress increases NPP/LA and LAI equally (Table 5). Nonetheless, the model underestimates the nitrogen limitation

15   of productivity at the 300yr site. The nitrogen capital of this site strongly depends on the nitrogen inputs and the efficiency at which nitrogen is retained in the ecosystem which we could only roughly approximate.

4   Conclusions

Here, we present the implementation of a terrestrial phosphorus cycle and its interactions with the carbon and nitrogen cycle into the land surface model ORCHIDEE. The model accounts for effects of nutrient stress on tissue nutrient concentration,

20   litter quality, root to shoot allocation and photosynthesis. We further account for root phosphorus uptake and the movement of phosphorus in the soil volume as an additional constraint on soil phosphorus availability to plants, to reduce the sensitivity of plant phosphorus availability to the sorption dynamics which can only be poorly constrained from available data (Goll et al., 2012; Reed et al., 2015).

We evaluated the performance of the model at two sites of contrasting nutrient availabilities (Crews et al., 1995; Harring-

25   ton et al., 2001; Ostertag, 2001). The model captures the different sensitivities of net primary productivity to nutrient addition among sites (Figure 4). It further tends to reproduce differences in the leaf area index and leaf level productivity between the alleviation of nitrogen and phosphorus stress (Table 5). As we prescribed a common parametrization ~~of vegetation characteristics~~ for all biological proccesses for both sites (Table 3), the contrasting response of vegetation to nutrient addition among sites is the emergent outcome of ~~the process representations governing the access and response of vegetation to changes in nutrient~~

30   ~~availability~~ differences in the physico-chemical soil characteristics.

The model shows some deficits which can be linked to the lack of plasticity in the allocation of new growth to the different plant tissues and biomass turnover - a common issue in global models (De Kauwe et al., 2014). It further underestimates nutrient use efficiencies in general primarily due to the overestimation of wood nutrient content and wood growth,

Table A1. Plant functional type (PFT) specific parameters: tropical evergreen broadleaf forest (TrEBF), tropical raingreen broadleaf forest (TrDBF), temperate evergreen needleleaf forest (TeENF), temperate evergreen broadleaf forest (TeEBF), temperate summergreen broadleaf forest (TeDBF), boreal evergreen needleleaf forest (BoENF), boreal summergreen broadleaf forest (BoDBF), boreal summergreen needleleaf forest (BoDNF), C3 grassland (C3grass), and C4 grassland (C4grass).

	TrEBF	TrDBF	TeENF	TeEBF	TeDBF	BoENF	BoDBF	BoDNF	C3grass	C4grass	Source
nue [μmol(CO_2)g^{-1}(N)s^{-1}]	22.	22.	20.	33.	33.	20.	33.	22.	45.	45.	Kattge et al. (2009)
$cn_{leaf,min}$ [g(C)g^{-1}(N)]	16.	16.	28.	16.	16.	28.	16.	16.	16.	16.	Zaehle and Friend (2010)
$cn_{leaf,max}$ [g(C)g^{-1}(N)]	60.	60.	75.	45.	45.	75.	45.	45.	45.	45.	Zaehle and Friend (2010)
$np_{leaf,min}$ [g(N)g^{-1}(P)]	16.68	16.68	8.34	10.84	10.84	8.34	10.84	10.84	10.84	10.84	McGroddy et al. (2004)
$np_{leaf,max}$ [g(N)g^{-1}(P)]	22.57	22.57	11.29	14.67	14.67	11.29	14.67	14.67	14.67	14.67	McGroddy et al. (2004)
λ_{root} [g(P)g^{-1}(P)]	1.	1.	1.	1.	1.	1.	1.	1.	1.	1.	Wang et al. (2010)
$\lambda_{sapwood}$ [g(P)g^{-1}(P)]	.087	.087	.087	.087	.087	.087	.087	.087	.087	.087	McGroddy et al. (2004); Sardans et al. (2015)

but we cannot rule out that the nitrogen use efficiency of photosynthesis in ORCHIDEE which is derived from data of plants growing on a wide range of soil nutrient availability (Kattge et al., 2009) does not apply to the extreme environment found during early and late stages of soil formation. ~~Further, we propose a mechanism by which the negative effect of drought on plant productivity is amplified in phosphorus poor environments. A trade-off between phosphorus acquisition and water transport seems plausible as the uptake of phosphorus requires are larger investment in specialized root systems which explore a larger volume of soil (Schachtman et al., 1998) due to immobility of phosphorus in soils, while uptake of water and mobile nutrient like nitrogen can be achieved by reducing root water pressure. Although, experimental findings indicate nutrient specific interactions between uptake of water and nutrient in tropical vegetation, current knowledge is insufficient (Lovelock et al., 2006; Cernusak et al., 2007; Santiago, 2015) to reject or support the proposed mechanism.~~

5 Code availability

The ORCHIDEE model version used here is a development branch of ORCHIDEE which is open source. The SVN version of the code branch is https://forge.ipsl.jussieu.fr/orchidee/browser/branches/ORCHIDEE-CN-P revision ~~3985 from the 17th January~~ 4520 from the 21st July 2017. Please contact the corresponding author for the code of the ORCHIDEE-CN-P if you plan an application of the model and envisage longer-term scientific collaboration.

6 Data availability

Primary data and scripts used in the analysis and other supplementary information that may be useful in reproducing the author's work can be obtained by contacting the corresponding author.

Table A2. Parameters of the dynamical weathering routine.

Parameter	Value	Units	Description	Source
s_{shield}	depends on location	–	soil shielding factor	Hartmann et al. (2014)
w_l	depends on location	g(P)mm	empirical factor	Hartmann et al. (2014)
a_l	depends on location	–	fraction of grid box occupied with lithology l	Hartmann and Moosdorf (2012)
$E_{a,l}$	depends on lithology	J	activation energy for lithological class l	Hartmann et al. (2014)
R	8.3144598	$Jmol^{-1}K^{-1}$	gas constant	
T_{ref}	284.15	K	reference temperature	Hartmann et al. (2014)

Table A3. Additional variables of the dynamical weathering routine.

Variable	Units	Description
$f_{tweath,l}$	–	temperature dependence of weathering
q_{ann}	$mmyr^{-1}$	annual sum of runoff and drainage
T_{2m}	K	2 meter air temperature
q	mmt^{-1}	sum of runoff and drainage

Table A4. The bias (simulated - observed) in carbon production per biomass nutrient (N_{prod},P_{prod}). From simulations (default) and as diagnosed by substituting simulated with observed nutrient content (observed xc_i) and/or biomass stocks (observed C_i).

	N_{prod} [%]		P_{prod} [%]	
	300yr	4.1Myr	300yr	4.1Myr
default	-59.4	-44.7	-20.0	+23.6
observed xc_i	-30.0	+33.2	-30.5	+26.2
observed C_i	-39.0	-62.9	-16.7	-25.6
observed C_i & xc_i	-0.6	-1.7	-0.6	-1.7

Table A5. The overall residence times of carbon (C_{MRT}), nitrogen (N_{MRT}) and phosphorus (P_{MRT}) in biomass (excluding storage), as well as the approximated residence time of all elements (C,N,P) in foliage ($X_{MRT,leaf}$), coarse roots and stems ($X_{MRT,wood}$), as well as fine roots ($X_{MRT,root}$). The latter three tissue classes consist of tissue with similar stoichiometry and thus the residence time of all element is ~~similar~~the same.

	300yr		4.1Myr	
	simulated	observed	simulated	observed
C_{MRT} [yr]	12.5	10.7	9.5	14.4
N_{MRT} [yr]	9.5	8.4	8.4	9.0
P_{MRT} [yr]	9.6	12.2	7.3	16.0
$X_{MRT,leaf}$ [yr]	2.1	1.6	1.8	1.6
$X_{MRT,root}$ [yr]	6.3	1.5	5.6	10.6
$X_{MRT,wood}$ [yr]	14.7	16.3	11.	18.1

Appendix A: Phosphorus release by chemical weathering

The release of phosphorus from minerals is the primary source of phosphorus for many terrestrial ecosystem. Besides pre-scribing release rates as done in this study, ORCHIDEE can simulate phosphorus release as a function of mineral phosphorus concentration, weatherability of minerals, intensity of the hydrological cycles as well as temperature (Hartmann and Moosdorf, 2012; Goll et al., 2014). All additional variables and parameters are found in Table A3&A2. The release of phosphorus from minerals is given by:

$$F_{weath} = s_{shield} \sum_{l=1,nl} f_{tweath,l} w_l a_l q_{ann} \tag{A1}$$

where s_{shield} is a scaling factor down-regulating release rates for soils where the active zone is disconnected from the bedrock, $f_{tweath,l}$ links the weathering reaction to temperature, w_l is an empirical parameter describing the P content and erodibility of lithological class l, a_l is the fraction of the grid-box occupied by lithological class l, and q_{ann} is a running average of the sum of drainage and surface runoff of the last 12 months.

The temperature dependence of weathering is described by an Arrhenius term (Hartmann et al., 2014):

$$f_{weath,l} = e^{(\frac{-E_{a,l}}{R})(\frac{1}{T_{2m}} - \frac{1}{T_{ref}})} \tag{A2}$$

where $E_{a,l}$ is the activation energy of the reaction for lithological class l, R is the gas constant, T_{2m} the long term (3 month) average of 2m air temperature, and T_{ref} the reference temperature.

This approach accounts for the hydrological constraint on the dissolution reaction by the removal of products as well as for the energetic constraints of the reaction itself (Hartmann et al., 2014). We take full advantage of the high resolution of the lithological data (Hartmann and Moosdorf, 2012) by assigning each ORCHIDEE grid box the fractional coverage of the

16 lithological classes thereby accounting for sub-grid scale heterogeneity in lithology. Following (Goll et al., 2014), we use 3 months running averages of the climatic drivers (q_{ann},T_{2m}). On that time scale, the soil temperature follows the 2m air temperature in most regions of the globe. This allows us to keep the original formulation which is based on air temperature. In soils where the active zone is disconnected from the bedrock the phosphorus release is down-regulated by a soil shielding

5 factor (s_l) which is read in from a global map (Hartmann et al., 2014).

Appendix B: Biological nitrogen fixation

While inputs of nitrogen from nitrogen-rich sedimentary rocks can make a significant contribution to the nitrogen budget of specific sites (Holloway, 2002; Morford et al., 2011), the major natural inputs are from biological fixation of atmospheric dinitrogen which is in ample supply (Vitousek et al., 2013). Biological nitrogen fixation (BNF) represents a key process which

10 can enhance nitrogen availability under elevated CO_2. Here we use a commonly used representation of BNF which is derived from an empirical correlation between BNF (F_{BNF}) and evapotranspiration (ET) (Cleveland et al., 1999) in which ET is substituted with NPP as they are highly correlated (Thornton et al., 2007):

$$F_{BNF} = \alpha_{bnf}(1 - e^{\beta_{BNF}NPP_{ann}}) \tag{B1}$$

where $\beta_{BNF} = -3 \times 10^{-3} \mathrm{yrg}^{-1}(C)$ is an empirical coefficients (Cleveland et al., 1999) and $\alpha_{bnf} = 0.967 \mathrm{g(N)yr}^{-1}$ was chosen

15 such that the global rate of BNF is close to an estimate of 58 $\mathrm{Tg(N)yr}^{-1}$ (Vitousek et al., 2013) for a NPP of 60 $\mathrm{Pg(C)yr}^{-1}$. We introduced a scaling function (f_{Nmin} to avoid unrealistic increases in BNF due to increases in NPP in case soil mineral nitrogen is in ample supply (Thomas et al., 2013).

$$F_{BNF} = c_{bnf}\alpha_{bnf}(1 - e^{\beta_{BNF}NPP_{ann}})f_{Nmin} \tag{B2}$$

where $c_{bnf} = 57.039 \times 10^{-6}$ is a factor to convert from the annual flux to a flux per time step, and NPP_{ann} is the running

20 average of the sum of net primary productivity during the last 12 months.

The scaling function f_{Nmin} is from Zaehle and Friend (2010) where it is used to the scale soil organic matter nitrogen content and given by:

$$f_{Nmin} = \begin{cases} (\frac{n_{th} - (N_{NH4} + N_{NO3}))}{n_{th}}) & \text{for}(N_{NH4} + N_{NO3}) < n_{th} \\ 0.0 & \text{otherwise} \end{cases} \tag{B3}$$

where n_{th} is a threshold of 2 $\mathrm{g(N)m}^{-2}$ and N_{Nh4} and N_{NO3} the respective concentrations of ammonia and of nitrate in the

25 soil.

Appendix C: Length correction for the spinup simulation of the 300yr old site

The 300yr site is characterized by low nitrogen availability due to the short period over which nitrogen could have accumulated via biological fixation and atmospheric deposition (Crews et al., 1995). In ORCHIDEE vegetation has to be initialized with

a minimum amount of biomass corresponding to a land cover with trees of an age between 2 and 3 yr (Naudts et al., 2015). The litter and soil organic matter pools are set to a negligible initial value. The minimum biomass corresponds to a substantial amount of total ecosystem nitrogen ($N_{tot}(0)$) of 20.8 g(N)m^{-2} being present at the end of the first year. Therefore, we reduce duration of the spinup simulation to compensate for the initial nitrogen stock.

5   To do so, we perform a 300 yr long simulation and estimate the fraction of nitrogen from biological nitrogen fixation and atmospheric deposition which is retained in the ecosystem (f_r):

$$f_r(t) = \frac{\Delta N_{tot}(t)}{BNF(t) + DEP_{obs}} \tag{C1}$$

where $\Delta N_{tot}(t)$ is the simulated annual change in N_{tot}, $BNF(t)$ is simulated annual flux of biological nitrogen and DEP_{obs} the annual flux of deposition (forcing) of year t We find that, besides during the first 40 yr, the $\overline{f_r}$ is with .11±.04 (average±standard

10   deviation) relatively constant. In combination with estimates of nitrogen fixation (BNF; gm^{-2}yr^{-1}) and atmospheric deposition (DEP; gm^{-2}yr^{-1}) the time (a) which would have been needed to accumulate the initial stock can be approximated by:

$$a = \frac{N_{tot}(t=0)}{\overline{f_r}(BNF_{obs} + DEP_{obs})} \tag{C2}$$

The observed rates of nitrogen fixation (BNF_{obs})during the first 150 yr of soil development in Hawaii are rather stable (2.0-3.1

15   g(N)m^{-2}yr^{-1}) (Crews et al., 2001), Estimates for atmospheric deposition (DEP_{obs}) are 0.6±0.4 g(N)m^{-2}yr^{-1} (Chadwick et al., 1999).

    Depending on f_r, 45–95yr would have been passed before 20.8 g(N)m^{-2} could have accumulated. We therefore, reduced the simulations duration from 300yr to 230yr.

    As the simulated NPP~~matches the observed NPP~~, biomass, and soil organic matter match the observation (Table 4) and the

20   dynamically simulated BNF rates are with 2.25 g(N)m^{-2}yr^{-1} well within the observed range, the reduction of the simulation length seems appropriate.

Appendix D: ~~soil phosphorus diffusion~~

~~In ORCHIDEE root phosphorus uptake and the soil permeability to phosphate ions are explicitly represented (Equation 4 & 22~~
~~). We aim to reduce the high sensitivity of plant phosphorus availability to the soil sorption coefficient (Goll et al., 2012) which~~

25   ~~cannot be sufficiently constrained from available observations, by introducing additional constraints on plant access to soil~~
~~phosphorus which can be constrained from experiments. Figure ?? shows the soil phosphorus concentration and plant uptake~~
~~for the year 2003 at the 4.1(phosphorus-limited) site. During dry periods, the phosphorus concentration at the root surface drops~~
~~to levels which are up to 50% lower than in the surrounding due the link between soil moisture and soil phosphorus permeability~~
~~in the model (Equation 24). As the concentration at the root surface declines plant uptake declines. We performed two additional~~

30   ~~simulations for the same year. In the first simulation the root zone concentration is set to the concentration of the surrounding~~
~~(Figure ??; broken line) which corresponds to the assumption of infinite soil permeability. In this simulation the annual~~

10 ~~constrained from available data and therefore are commonly subject to calibration.~~

Appendix D: Analysis of biases in carbon production rate per biomass nutrient

Here we investigate the cause of the model biases in carbon productivity of nutrient x (X_{prod}). All calculation are done with the long-term averages of the simulated variables and not with the annual fluxes like done in the main analysis. Thus the values might deviate slightly from the ones reported earlier. By substituting $N_{content}$ in Equation 30 with the carbon mass of tissue i

15 and the respective x:c ratios (xc_i) we can investigate the contribution of the respective components of X_{prod} to the overall bias in X_{prod}:

$$X_{prod} = \frac{NPP}{\sum C_i xc_i} \tag{D1}$$

To calculate the contribution of the bias in nc_i to the bias in N_{prod}, we used simulated nc_i but NPP and C_i from observation in Equation D1.

20 We find that at both sites the underestimation of N_{prod} of -59.4% and 44.7% are related to the overestimation of tissue nitrogen content (see "observed C_i" in Table A4). The effect of biases in simulated biomass on N_{prod} differs between sites, as biomass stocks, and subsequently nitrogen stocks, are underestimated at the 300yr site while they are overestimated at the 4.1Myr site (Figure 3). When biomass and nitrogen content are taken from observation the bias in N_{prod} are in general low due to the good agreement of simulated and observed NPP (Figure 3).

25 The effect of biases in xc_i and/or C_i on P_{prod} are comparable to their effects on N_{prod} at both sites.

We calculated the residence time of nutrients ($X_{MRT,i}$) for classes of tissues with sharing similar stoichiometry in OR-CHIDEE, namely leaf, coarse root and stems, and fine roots:

$$X_{MRT,i} = \frac{C_i xc_i}{NPP_i xc_i} \tag{D2}$$

where NPP_i is the fraction of NPP being allocated to tissue class i. The equation can be simplified to:

30 $$X_{MRT,i} = \frac{C_i}{NPP_i} \tag{D3}$$

showing that the residence time $X_{MRT,i}$ equals to the residence time of carbon. Table A5 shows the residence times of the different tissue classes as well as C_{MRT}, N_{MRT}, and P_{MRT} calculated as described in the method section of the main manuscript.

The observed residence times of carbon, nitrogen and phosphorus (Table A5) are longer at the 4.1Myr than they are at the
5 300yr site, whereas the model simulates an opposite pattern. As the constant tissue turnover rates are used in ORCHIDEE the model is not able to reproduce differences among sites. The slightly longer residence times at the young site can be attributed to the transient state of vegetation in which it is still accumulating biomass, while the biomass at the old site reached a stable state. The model consistently underestimates the residence time of phosphorus P_{MRT}, which can be attributed to an underestimation of the phosphorus content of stems and coarse roots (not shown).

Competing interests. The authors declare that they have no conflict of interest.

References

Amazon Fertilization Experiment (AFEX), https://amazonfertilisationexperiment.wordpress.com.

AmazonFACE, https://amazonface.org/.

EucFACE, https://www.westernsydney.edu.au/hie/facilities/EucFACE.

5 Effects of phosphorus limitations on Life, Earth system and Society (IMBALANCE-P), http://imbalancep-erc.creaf.cat/.

Quantifying the effects of interacting nutrient cycles on terrestrial biosphere dynamics and their climate feedbacks (QUINCY), https://www.
bgc-jena.mpg.de/bgi/index.php/Projects/QUINCY.

Forest Strategies for limited Phosphorus Resources (SPP1685), www.ecosystem-nutrition.uni-freiburg.de.

Ali, a. a., Xu, C., Rogers, A., Fisher, R. a., Wullschleger, S. D., McDowell, N. G., Massoud, E. C., Vrugt, J. a., Muss, J. D., Fisher, J. B., Reich,
10 P. B., and Wilson, C. J.: A global scale mechanistic model of the photosynthetic capacity, Geosci. Model Dev. Discuss., 8, 6217–6266,
doi:10.5194/gmdd-8-6217-2015, http://www.geosci-model-dev-discuss.net/8/6217/2015/, 2015.

Bahar, N. H. A., Ishida, F. Y., Weerasinghe, L. K., Guerrieri, R., O'Sullivan, O. S., Bloomfield, K. J., Asner, G. P., Martin, R. E., Lloyd, J.,
Malhi, Y., Phillips, O. L., Meir, P., Salinas, N., Cosio, E. G., Domingues, T. F., Quesada, C. A., Sinca, F., Escudero Vega, A., Zuloaga
Ccorimanya, P. P., del Aguila-Pasquel, J., Quispe Huaypar, K., Cuba Torres, I., Butrón Loayza, R., Pelaez Tapia, Y., Huaman Ovalle, J.,
15 Long, B. M., Evans, J. R., and Atkin, O. K.: Leaf-level photosynthetic capacity in lowland Amazonian and high-elevation Andean tropical
moist forests of Peru, New Phytol., doi:10.1111/nph.14079, 2016.

BARRACLOUGH, P. B. and TINKER, P. B.: The Determination of Ionic Diffusion Coefficients in Field Soils. I. Diffusion Coefficients in
Sieved Soils in Relation To Water Content and Bulk Density, J. Soil Sci., 32, 225–236, doi:10.1111/j.1365-2389.1981.tb01702.x, 1981.

Barron, A. R., Wurzburger, N., Bellenger, J. P., Wright, S. J., Kraepiel, A. M. L., and Hedin, L. O.: Molybdenum limitation of asymbiotic
20 nitrogen fixation in tropical forest soils, Nat. Geosci., 2, 42–45, doi:10.1038/ngeo366, http://dx.doi.org/10.1038/ngeo366, 2009.

Bonan, G. B., Williams, M., Fisher, R. A., and Oleson, K. W.: Modeling stomatal conductance in the earth system: Linking leaf water-use
efficiency and water transport along the soil-plant-atmosphere continuum, Geosci. Model Dev., 7, 2193–2222, doi:10.5194/gmd-7-2193-
2014, 2014.

Bouma, T. J., Yanai, R. D., Elkin, A. D., Hartmond, U., Flores-Alva, D. E., and Eissenstat, D. M.: Estimating age-dependent costs and benefits
25 of roots with contrasting life span: Comparing apples and oranges, New Phytol., 150, 685–695, doi:10.1046/j.1469-8137.2001.00128.x,
2001.

Brovkin, V. and Goll, D.: Land unlikely to become large carbon source, Nat. Geosci, 8, 893, doi:10.1038/ngeo2598, http://dx.doi.org/10.
1038/ngeo2598{%}5Cn10.1038/ngeo2598, 2015.

Campo, J. and Dirzo, R.: Leaf quality and herbivory responses to soil nutrient addition in secondary tropical dry forests of Yucatán, Mexico,
30 J. Trop. Ecol., 19, 525–530, doi:10.1017/S0266467403003572, 2003.

Casotti, G. and Bradley, J. S.: Leaf nitrogen and its effects on the rate of herbivory on selected eucalypts in the jarrah forest, For. Ecol.
Manage., 41, 167–177, doi:10.1016/0378-1127(91)90101-Z, 1991.

Cernusak, L. A., Winter, K., Aranda, J., Turner, B. L., and Marshall, J. D.: Transpiration efficiency of a tropical pioneer tree (Ficus insipida)
in relation to soil fertility, J. Exp. Bot., 58, 3549–3566, doi:10.1093/jxb/erm201, 2007.

35 Chadwick, O. A., Derry, L. A., Vitousek, P. M., Huebert, B. J., and Hedin, L. O.: Changing sources of nu-
trients during four million years of ecosystem development, Nature, 397, 491–497, http://file//localhost(null)
{%}5Cnpapers3://publication/uuid/7ECD2681-24EA-40C4-BC40-6A9C53752C0B{%}5Cnpapers3://publication/uuid/

25FAA339-824E-4065-8609-F771989E96F6{%}5Cnpapers3://publication/uuid/E18FAB50-A6E2-4AC7-B336-1451CD393E25{%}5Cnpapers3: //publication/, 1999.

Chorover, J., Amistadi, M. K., and Chadwick, O. A.: Surface charge evolution of mineral-organic complexes during pedogenesis in Hawaiian basalt, Geochim. Cosmochim. Acta, 68, 4859–4876, doi:10.1016/j.gca.2004.06.005, 2004.

5   Cleveland, C. C., Townsend, A. R., Schimel, D. S., Fisher, H., Hedin, L. O., Perakis, S., Latty, E. F., Fischer, C. V., Elseroad, A., and Wasson, M. F.: Global patterns of terrestrial biological nitrogen (N2) fixation in natural ecosystems, Glob. Biochem. Cycles, 13, 623–645, doi:10.1029/1999GB900014, http://onlinelibrary.wiley.com/doi/10.1029/1999GB900014/pdf, 1999.

Crews, T. E., Kitayama, K., Fownes, J. H., Riley, R. H., Darrell, A., Mueller-dombois, D., and Vitousek, P. M.: Changes in Soil Phosphorus Fractions and Ecosystem Dynamics across a Long Chronosequence in Hawaii, Ecology, 76, 1407–1424, 1995.

10   Crews, T. E., Kurina, L. M., and Vitousek, P. M.: Organic matter and nitrogen accumulation and nitrogen fixation during early ecosystem development in Hawaii, Biogeochemistry, 52, 259–279, doi:10.1023/A:1006441726650, http://link.springer.com/article/10.1023/A: 1006441726650{%}5Cnpapers2://publication/uuid/2D8B1F81-45CD-4265-8B45-A79BF51643FF, 2001.

De Kauwe, M. G., Medlyn, B. E., Zaehle, S., Walker, A. P., Dietze, M. C., Wang, Y.-P., Luo, Y., Jain, A. K., El-Masri, B., Hickler, T., Wårlind, D., Weng, E., Parton, W. J., Thornton, P. E., Wang, S., Prentice, I. C., Asao, S., Smith, B., McCarthy, H. R., Iversen, C. M.,
15   Hanson, P. J., Warren, J. M., Oren, R., and Norby, R. J.: Where does the carbon go? A model-data intercomparison of vegetation carbon allocation and turnover processes at two temperate forest free-air CO2 enrichment sites., New Phytol., doi:10.1111/nph.12847, http: //www.ncbi.nlm.nih.gov/pubmed/24844873, 2014.

Doetterl, S., Stevens, A., Six, J., Merckx, R., Oost, K. V., Pinto, M. C., Casanova-katny, A., Muñoz, C., Boudin, M., Venegas, E. Z., and Boeckx, P.: Soil carbon storage controlled by interactions between geochemistry and climate, Nat. Geosci., 8, 780–783,
20   doi:10.1038/NGEO2516, 2015.

Domingues, T. F., Meir, P., Feldpausch, T. R., Saiz, G., Veenendaal, E. M., Schrodt, F., Bird, M., Djagbletey, G., Hien, F., Compaore, H., Diallo, A., Grace, J., and Lloyd, J.: Co-limitation of photosynthetic capacity by nitrogen and phosphorus in West Africa woodlands, Plant, Cell Environ., 33, 959–980, doi:10.1111/j.1365-3040.2010.02119.x, 2010.

Finzi, A. C., Norby, R. J., Calfapietra, C., Gallet-Budynek, A., Gielen, B., Holmes, W. E., Hoosbeek, M. R., Iversen, C. M., Jackson, R. B.,
25   Kubiske, M. E., Ledford, J., Liberloo, M., Oren, R., Polle, A., Pritchard, S., Zak, D. R., Schlesinger, W. H., and Ceulemans, R.: Increases in nitrogen uptake rather than nitrogen-use efficiency support higher rates of temperate forest productivity under elevated CO2., Proc. Natl. Acad. Sci. U. S. A., 104, 14 014–14 019, doi:10.1073/pnas.0706518104, 2007.

Fox, T. R.: Rhizosphere Activity and Organic Phosphorus in Two Forested, Soil Biol. Biochem., 24, 579–583, 1992.

Goddéris, Y., François, L. M., Probst, A., Schott, J., Moncoulon, D., Labat, D., and Viville, D.: Modelling weathering processes at the
30   catchment scale: The WITCH numerical model, Geochim. Cosmochim. Acta, 70, 1128–1147, doi:10.1016/j.gca.2005.11.018, 2006.

Goll, D. S., Brovkin, V., Parida, B. R., Reick, C. H., Kattge, J., Reich, P. B., Van Bodegom, P. M., and Niinemets, Ü.: Nutrient limitation reduces land carbon uptake in simulations with a model of combined carbon, nitrogen and phosphorus cycling, Biogeosciences, 9, 3547– 3569, doi:10.5194/bg-9-3547-2012, http://www.biogeosciences.net/9/3547/2012/, 2012.

Goll, D. S., Moosdorf, N., Hartmann, J., and Brovkin, V.: Climate-driven changes in chemical weathering and associated phosphorus release
35   since 1850: Implications for the land carbon balance, Geophys. Res. Lett., 41, 3553–3558, doi:10.1002/2014GL059471, http://doi.wiley. com/10.1002/2014GL059471, 2014.

Harrington, R. A., Fownes, J. H., and Vitousek, P. M.: Production and resource use efficiencies in N- and P-limited tropical forests: A comparison of responses to long-term fertilization, Ecosystems, 4, 646–657, doi:10.1007/s10021-001-0034-z, 2001.

Harris, I., Jones, P. D., Osborn, T. J., and Lister, D. H.: Updated high-resolution grids of monthly climatic observations – the CRU TS3.10, Int. J. Clim., 34, 623–642, 2014.

Hartmann, H. and Trumbore, S.: Understanding the roles of nonstructural carbohydrates in forest trees - from what we can measure to what we want to know, New Phytol., doi:10.1111/nph.13955, http://doi.wiley.com/10.1111/nph.13955, 2016.

5   Hartmann, J. and Moosdorf, N.: The new global lithological map database GLiM: A representation of rock properties at the Earth surface, Geochem. Geophys. Geosyst., 13, 1–37, doi:10.1029/2012GC004370, http://doi.wiley.com/10.1029/2012GC004370, 2012.

Hartmann, J., Moosdorf, N., Lauerwald, R., Hinderer, M., and West, A. J.: Global chemical weathering and associated p-release - the role of lithology, temperature and soil properties, Chem. Geol., 363, 145–163, doi:10.1016/j.chemgeo.2013.10.025, http://linkinghub.elsevier.com/retrieve/pii/S0009254113004816, 2014.

10 Heineman, K. D., Turner, B. L., and Dalling, J. W.: Variation in wood nutrients along a tropical soil fertility gradient, New Phytol., doi:10.1111/nph.13904, 2016.

Hofmann, K., Heuck, C., and Spohn, M.: Phosphorus resorption by young beech trees and soil phosphatase activity as dependent on phosphorus availability, Oecologia, 181, 369–379, doi:10.1007/s00442-016-3581-x, 2016.

Holloway, J. M.: Nitrogen in rock: Occurrences and biogeochemical implications, Global Biogeochem. Cycles, 16, 65–1–65–17,
15 doi:10.1029/2002GB001862, http://doi.wiley.com/10.1029/2002GB001862, 2002.

Ichie, T. and Nakagawa, M.: Dynamics of mineral nutrient storage for mast reproduction in the tropical emergent tree Dryobalanops aromatica., Ecol. Res., 28, 151–158, doi:DOI: 10.1007/s11284-011-0836-1, 2013.

Johnson, A. H., Frizano, J., Vann, D. R., and Johnson, R. A. H.: Biogeochemical implications of labile phosphorus in forest soils determined by the Hedley fractionation procedure, Oecologia, 135, 487–499, doi:10.1007/s00442-002-1164-5, 2003.

20 Johnson, I. R. I. and Thornley, J.: A model of instantaneous and daily canopy photosynthesis, J. Theor. Biol., 107, 531–545, doi:10.1016/S0022-5193(84)80131-9, 1984.

Kattge, J. and Knorr, W.: Temperature acclimation in a biochemical model of photosynthesis: a reanalysis of data from 36 species, PLANT CELL Environ., 30, 1176–1190, doi:10.1111/j.1365-3040.2007.01690.x, 2007.

Kattge, J., Knorr, W., Raddatz, T., and Wirth, C.: Quantifying photosynthetic capacity and its relationship to leaf nitrogen content for global-
25 scale terrestrial biosphere models, Glob. Chang. Biol., 15, 976–991, doi:10.1111/j.1365-2486.2008.01744.x, 2009.

KATTGE, J., DÍAZ, S., LAVOREL, S., PRENTICE, I. C., LEADLEY, P., BÖNISCH, G., GARNIER, E., WESTOBY, M., REICH, P. B., WRIGHT, I. A. N. J., CORNELISSEN, J. H. C., VIOLLE, C., HARRISON, S. P., van BODEGOM, P. M., REICHSTEIN, M., ENQUIST, B. J., SOUDZILOVSKAIA, N. A., ACKERLY, D. D., ANAND, M., ATKIN, O., BAHN, M., BAKER, T. R., BALDOCCHI, D., BEKKER, R., BLANCO, C. C., BLONDER, B., BOND, W. J., BRADSTOCK, R., BUNKER, D. E., CASANOVES, F., CAVENDER-BARES, J.,
30 CHAMBERS, J. Q., CHAPIN, F. S., CHAVE, J., COOMES, D., CORNWELL, W. K., CRAINE, J. M., DOBRIN, B. H., DUARTE, L., DURKA, W., ELSER, J., ESSER, G., ESTIARTE, M., FAGAN, W. F., FANG, J., FERNÁNDEZ-MÉNDEZ, F., FIDELIS, A., FINEGAN, B., FLORES, O., FORD, H., FRANK, D., FRESCHET, G. T., FYLLAS, N. M., GALLAGHER, R. V., GREEN, W. A., GUTIERREZ, A. G., HICKLER, T., HIGGINS, S., HODGSON, J. G., JALILI, A., JANSEN, S., JOLY, C., KERKHOFF, A. J., KIRKUP, D. O. N., KITAJIMA, K., KLEYER, M., KLOTZ, S., KNOPS, J. M. H., KRAMER, K., KÜHN, I., KUROKAWA, H., LAUGHLIN, D., LEE,
35 T. D., LEISHMAN, M., LENS, F., LENZ, T., LEWIS, S. L., LLOYD, J. O. N., LLUSIÀ, J., LOUAULT, F., MA, S., MAHECHA, M. D., MANNING, P., MASSAD, T., MEDLYN, B., MESSIER, J., MOLES, A. T., MÜLLER, S. C., NADROWSKI, K., NAEEM, S., NIINEMETS, Ü. L. O., NÖLLERT, S., NÜSKE, A., OGAYA, R., OLEKSYN, J., ONIPCHENKO, V. G., ONODA, Y., ORDOÑEZ, J., OVERBECK, G., OZINGA, W. I. M. A., PATIÑO, S., PAULA, S., PAUSAS, J. G., PEÑUELAS, J., PHILLIPS, O. L., PILLAR, V.,

35

POORTER, H., POORTER, L., POSCHLOD, P., PRINZING, A., PROULX, R., RAMMIG, A., REINSCH, S., REU, B., SACK, L., SALGADO-NEGRET, B., SARDANS, J., SHIODERA, S., SHIPLEY, B., SIEFERT, A., SOSINSKI, E., SOUSSANA, J.-F., SWAINE, E., SWENSON, N., THOMPSON, K. E. N., THORNTON, P., WALDRAM, M., WEIHER, E., WHITE, M., WHITE, S., WRIGHT, S. J., YGUEL, B., ZAEHLE, S., ZANNE, A. M. Y. E., and WIRTH, C.: TRY – a global database of plant traits, Glob. Chang. Biol., pp. no—-no, doi:10.1111/j.1365-2486.2011.02451.x, http://dx.doi.org/10.1111/j.1365-2486.2011.02451.x, 2011.

Kirschbaum, M. U. F., Simioni, G., Medlyn, B. E., and McMurtrie, R. E.: On the importance of including soil nutrient feedback effects for predicting ecosystem carbon exchange, Funct. Plant Biol., 30, 223, doi:10.1071/FP02152, http://www.publish.csiro.au/?paper=FP02152, 2003.

Koerselman, W. and Meuleman, A. F. M. A.: The Vegetation N:P Ratio: a New Tool to Detect the Nature of Nutrient Limitation, J. Appl. Ecol., 33, 1441–1450, doi:10.2307/2404783, http://www.jstor.org/stable/10.2307/2404783{%}5Cnhttp://www.jstor.org/stable/2404783, 1996.

Krinner, G., Viovy, N., de Noblet-Ducoudré, N., Ogée, J., Polcher, J., Friedlingstein, P., Ciais, P., Sitch, S., and Prentice, I. C.: A dynamic global vegetation model for studies of the coupled atmosphere-biosphere system, Global Biogeochem. Cycles, 19, n/a–n/a, doi:10.1029/2003GB002199, http://doi.wiley.com/10.1029/2003GB002199, 2005.

Kronzucker, H. J., Siddiqi, M. Y., and Glass, A. D. M.: Kinetics of NO Influx in Spruce, Plant Physiol., 109, 319–326, 1995.

Lawrence, D.: Nitrogen and Phosphorus Enhance Growth and Luxury Consumption of Four Secondary Forest Tree Species in Borneo Author (s): Deborah Lawrence Published by : Cambridge University Press Stable URL : http://www.jstor.org/stable/3068619 REFERENCES Linked refer, J. Trop. Ecol., 17, 859–869, 2001.

Li, X. L., George, E., and Marschner, H.: Extension of the phosphorus depletion zone in VA-mycorrhizal white clover in a calcareous soil, Plant Soil, 136, 41–48, doi:10.1007/BF02465219, 1991.

Lovelock, C. E., Ball, M. C., Choat, B., Engelbrecht, B. M. J., Holbrook, N. M., and Feller, I. C.: Linking physiological processes with mangrove forest structure: Phosphorus deficiency limits canopy development, hydraulic conductivity and photosynthetic carbon gain in dwarf Rhizophora mangle, Plant, Cell Environ., 29, 793–802, doi:10.1111/j.1365-3040.2005.01446.x, 2006.

Marotzke, J., Jakob, C., Bony, S., Dirmeyer, P. A., O'Gorman, P. A., Hawkins, E., Perkins-Kirkpatrick, S., Quéré, C. L., Nowicki, S., Paulavets, K., Seneviratne, S. I., Stevens, B., and Tuma, M.: Climate research must sharpen its view, Nat. Clim. Chang., doi:10.1038/nclimate3206, http://www.nature.com/doifinder/10.1038/nclimate3206, 2017.

McGechan, M. and Lewis, D.: Sorption of Phorphorus by Soil, Part 1: Principles, Equations and Models, Biosyst. Eng., 82, 1–24, doi:10.1006/bioe.2002.0054, http://linkinghub.elsevier.com/retrieve/pii/S1537511002900541, 2002.

McGill, W. B. and Cole, C. V.: Comparative aspects of cycling of organic C, N , S, and P through soil organic matter, Geoderma, 26, 267–268, 1981.

McGroddy, M. E., Daufresne, T., and Hedin, L. O.: Scaling of C:N:P stoichiometry in forest worldwide: implications of terrestrial redfield-like ratios, Ecology, 85, 2390–2401, 2004.

Medlyn, B. E., Kauwe, M. G. D., Walker, A. P., Dietze, C., Hanson, P., Hickler, T., Jain, A., Luo, Y., Parton, W., Colin, I., Wang, S., Wang, Y.-p., Weng, E., Iversen, C. M., Mccarthy, H., Warren, J., Oren, R., Norby, R., Division, E. S., Ridge, O., Goethe, G., and Collins, F.: Using Ecosystem Experiments to Improve Vegetation Models : Lessons Learnt from the Free-Air CO 2 Enrichment Model-Data Synthesis, Nat. Clim. Chang., 5, 528–534, doi:10.1038/nclimate2621, 2015.

Meyerholt, J. and Zaehle, S.: The role of stoichiometric flexibility in modelling forest ecosystem responses to nitrogen fertilization, New Phytol., 208, 1042–1055, doi:10.1111/nph.13547, 2015.

Mollier, A., De Willigen, P., Heinen, M., Morel, C., Schneider, A., and Pellerin, S.: A two-dimensional simulation model of phosphorus uptake including crop growth and P-response, Ecol. Modell., 210, 453–464, doi:10.1016/j.ecolmodel.2007.08.008, 2008.

Mooshammer, M., Wanek, W., Hämmerle, I., Fuchslueger, L., Hofhansl, F., Knoltsch, A., Schnecker, J., Takriti, M., Watzka, M., Wild, B., Keiblinger, K. M., Zechmeister-Boltenstern, S., and Richter, A.: Adjustment of microbial nitrogen use efficiency to carbon:nitrogen imbalances regulates soil nitrogen cycling., Nat. Commun., 5, 3694, doi:10.1038/ncomms4694, http://www.pubmedcentral.nih.gov/articlerender.fcgi?artid=3997803{&}tool=pmcentrez{&}rendertype=abstract, 2014.

Morford, S. L., Houlton, B. Z., and Dahlgren, R. a.: Increased forest ecosystem carbon and nitrogen storage from nitrogen rich bedrock., Nature, 477, 78–81, doi:10.1038/nature10415, http://www.nature.com/nature/journal/v477/n7362/full/nature10415.html?WT.ec{_}i.., 2011.

Naudts, K., Ryder, J., McGrath, M. J., Otto, J., Chen, Y., Valade, A., Bellasen, V., Berhongaray, G., B??nisch, G., Campioli, M., Ghattas, J., De Groote, T., Haverd, V., Kattge, J., MacBean, N., Maignan, F., Merila??, P., Penuelas, J., Peylin, P., Pinty, B., Pretzsch, H., Schulze, E. D., Solyga, D., Vuichard, N., Yan, Y., and Luyssaert, S.: A vertically discretised canopy description for ORCHIDEE (SVN r2290) and the modifications to the energy, water and carbon fluxes, Geosci. Model Dev., 8, 2035–2065, doi:10.5194/gmd-8-2035-2015, 2015.

Niu, Y. F., Chai, R. S., Jin, G. L., Wang, H., Tang, C. X., and Zhang, Y. S.: Responses of root architecture development to low phosphorus availability: A review, Ann. Bot., 112, 391–408, doi:10.1093/aob/mcs285, 2013.

Norby, R. J., Gu, L., Haworth, I. C., Jensen, A. M., Turner, B. L., Walker, A. P., Warren, J. M., Weston, D. J., Xu, C., and Winter, K.: Informing models through empirical relationships between foliar phosphorus, nitrogen and photosynthesis across diverse woody species in tropical forests of Panama, New Phytol., doi:10.1111/nph.14319, http://doi.wiley.com/10.1111/nph.14319, 2016.

Olander, L. P. and Vitousek, P. M.: Regulation of soil phosphatase and chitinase activity by N and P availability, Biogeochemistry, 49, 175–190, doi:10.1023/A:1006316117817, 2000.

Olander, L. P. and Vitousek, P. M.: Biological and Geochemical Sinks for Phosphorus in Soil from a Wet Tropical Forest, Ecosystems, 7, 404–419, doi:10.1007/s10021-004-0264-y, http://springerlink.metapress.com/openurl.asp?genre=article{&}id=doi:10.1007/s10021-004-0264-y, 2004.

Olesen, T., Moldrup, P., Yamaguchi, T., and Rolston, D. E.: Constant slope impedance factor model for predicting the solute diffusion coefficient in unsaturated soil, Soil Sci., 166, 89–96, doi:10.1097/00010694-200102000-00002, 2001.

Ostertag, R. E. O.: Fine-Root Dynamics in Hawaiian Montane Forests, Ecology, 82, 485–499, 2001.

Parton, W. J., Scurlock, J. M. O., Ojima, D. S., Gilmanov, T. G., Scholes, R. J., Schimel, D. S., Kirchner, T., Menaut, J.-C., Seastedt, T. R., Garcia Moya, E., Kamnalrut, A., and Kinyamario, J. I.: Observations and modeling of biomass and soil organic matter dynamics for the grassland biome worldwide, Global Biogeochem. Cycles, 7, 785–809, doi:10.1029/93GB02042, 1993.

Peñuelas, J., Poulter, B., Sardans, J., Ciais, P., van der Velde, M., Bopp, L., Boucher, O., Godderis, Y., Hinsinger, P., Llusia, J., Nardin, E., Vicca, S., Obersteiner, M., and Janssens, I. a.: Human-induced nitrogen-phosphorus imbalances alter natural and managed ecosystems across the globe., Nat. Commun., 4, 2934, doi:10.1038/ncomms3934, http://www.ncbi.nlm.nih.gov/pubmed/24343268, 2013.

Piper, F. I. and Fajardo, A.: Foliar habit, tolerance to defoliation and their link to carbon and nitrogen storage, J. Ecol., 102, 1101–1111, doi:10.1111/1365-2745.12284, 2014.

Reed, S. C., Yang, X., and Thornton, P. E.: Incorporating phosphorus cycling into global modeling efforts: A worthwhile, tractable endeavor, New Phytol., 208, 324–329, doi:10.1111/nph.13521, 2015.

Reich, P. B., Oleksyn, J., and Wright, I. J.: Leaf phosphorus influences the photosynthesis-nitrogen relation: A cross-biome analysis of 314 species, Oecologia, 160, 207–212, doi:10.1007/s00442-009-1291-3, 2009.

Santiago, L. S.: Nutrient limitation of eco-physiological processes in tropical trees, Trees, 29, 1291–1300, doi:10.1007/s00468-015-1260-x, http://link.springer.com/10.1007/s00468-015-1260-x, 2015.

Sardans, J., Janssens, I. A., Alonso, R., Veresoglou, S. D., Rillig, M. C., Sanders, T. G., Carnicer, J., Filella, I., Farré-Armengol, G., and Peñuelas, J.: Foliar elemental composition of European forest tree species associated with evolutionary traits and present environmental and competitive conditions, Glob. Ecol. Biogeogr., 24, 240–255, doi:10.1111/geb.12253, http://doi.wiley.com/10.1111/geb.12253, 2015.

Schachtman, D. P., Reid, R. J., Ayling, S. M., S, D. B. D. P., and A, S. S. S. M.: Phosphorus Uptake by Plants: From Soil to Cell, Plant Physiol., 116, 447–453, 1998.

Shcherbak, I., Millar, N., and Robertson, G. P.: Global metaanalysis of the nonlinear response of soil nitrous oxide (N2O) emissions to fertilizer nitrogen, Proc. Natl. Acad. Sci., 111, 9199–9204, doi:10.1073/pnas.1322434111, http://www.pnas.org/content/111/25/9199.abstract, 2014.

Shinozaki, K., Yoda, K., Hozumi, K., and Kira, T.: A quantitative analysis of plant form - the pipe model theory: I Basix analysis, Jpn. J. Ecol., 14, 97–105, 1964.

Smith, B., Wårlind, D., Arneth, A., Hickler, T., Leadley, P., Siltberg, J., and Zaehle, S.: Implications of incorporating N cycling and N limitations on primary production in an individual-based dynamic vegetation model, Biogeosciences, 11, 2027–2054, doi:10.5194/bg-11-2027-2014, http://www.biogeosciences.net/11/2027/2014/, 2014.

Spohn, M. and Kuzyakov, Y.: Phosphorus mineralization can be driven by microbial need for carbon, Soil Biol. Biochem., 61, 69–75, doi:10.1016/j.soilbio.2013.02.013, http://dx.doi.org/10.1016/j.soilbio.2013.02.013, 2013.

Stewart, J. W. B. and Tiessen, H.: DYynamics of soil organic phosphorus, Biogeochemistry, 4, 41–60, doi:10.1007/BF02187361, 1987.

Thomas, R. Q., Zaehle, S., Templer, P. H., and Goodale, C. L.: Global patterns of nitrogen limitation: Confronting two global biogeochemical models with observations, Glob. Chang. Biol., 19, 2986–2998, doi:10.1111/gcb.12281, 2013.

Thornton, P., Thornton, M., and Vose, R.: Daymet V3: Annual Tile Summary Cross-Validation Statistics for North America, Hawaii, Tech. rep., ORNL DAAC, Oak Ridge, Tennessee, USA., doi:http://dx.doi.org/10.3334/ORNLDAAC/1348, 2016.

Thornton, P. E., Rosenbloom, N. a., Mahowald, N. M., Lamarque, J. F. J.-F., Rosenbloom, N. a., and Mahowald, N. M.: Influence of carbon-nitrogen cycle coupling on land model response to CO2 fertilization and climate variability, Global Biogeochem. Cycles, 21, 1–15, doi:10.1029/2006GB002868, 2007.

Tipping, E., Somerville, C. J., and Luster, J.: The C:N:P:S stoichiometry of soil organic matter, Biogeochemistry, pp. 117–131, doi:10.1007/s10533-016-0247-z, http://link.springer.com/10.1007/s10533-016-0247-z, 2016.

Van Wijk, M. T., Williams, M., Cough, L., Hobbie, S. E., and Shaver, G. R.: Luxury consumption of soil nutrients: a possible competitive strategy in \rabove-ground and below-ground biomass allocation and root morphology for \rslow-growing arctic vegetation?, J. Ecol., pp. 664–676, doi:10.1046/j.1365-2745.2003.00788.x, c:{%}5CPDFs{%}5Cj.1365-2745.2003.00788.x.pdf, 2003.

Verheijen, L. M., Aerts, R., Bönisch, G., Kattge, J., and Van Bodegom, P. M.: Variation in trait trade-offs allows differentiation among predefined plant functional types: Implications for predictive ecology, New Phytol., 209, 563–575, doi:10.1111/nph.13623, 2016.

Vitousek, P. M.: Nutrient Cycling and Limitation: Hawaii as a Model System, Princeton University Press, Princeton, N.J., U.S.A., 2004.

Vitousek, P. M., Menge, D. N. L., Reed, S. C., and Cleveland, C. C.: Biological nitrogen fixation: rates, patterns and ecological controls in terrestrial ecosystems., Philos. Trans. R. Soc. Lond. B. Biol. Sci., 368, 20130 119, doi:10.1098/rstb.2013.0119, http://www.ncbi.nlm.nih.gov/pubmed/23713117, 2013.

Walker, A. P., Beckerman, A. P., Gu, L., Kattge, J., Cernusak, L. a., Domingues, T. F., Scales, J. C., Wohlfahrt, G., Wullschleger, S. D., and Woodward, F. I.: The relationship of leaf photosynthetic traits - V cmax and J max - to leaf nitrogen, leaf phosphorus, and specific leaf area: a meta-analysis and modeling study, Ecol. Evol., pp. n/a–n/a, doi:10.1002/ece3.1173, http://doi.wiley.com/10.1002/ece3.1173, 2014.

5 Walker, A. P., Zaehle, S., Medlyn, B. E., De Kauwe, M. G., Asao, S., Hickler, T., and Norby, R. J.: Predicting long-term carbon sequestration in response to CO2 enrichment: How and why do current ecosystem models differ?, Global Biogeochem. Cycles, 5, 1–20, doi:10.1002/2014GB004995.Received, 2015.

Walker, T. W. and Syers, J. K.: The fate of phosphorus during pedogenesis, Geoderma, 15, 1–19, doi:10.1016/0016-7061(76)90066-5, http://linkinghub.elsevier.com/retrieve/pii/0016706176900665, 1976.

Wang, F., Cheruy, F., and Dufresne, J. L.: The improvement of soil thermodynamics and its effects on land surface meteorology in the IPSL
10 climate model, Geosci. Model Dev., 9, 363–381, doi:10.5194/gmd-9-363-2016, 2016.

Wang, Y.-P., Houlton, B. Z., and Field, C. B.: A model of biogeochemical cycles of carbon, nitrogen, and phosphorus including symbiotic nitrogen fixation and phosphatase production, Global Biogeochem. Cycles, 21, n/a–n/a, doi:10.1029/2006GB002797, http://doi.wiley.com/10.1029/2006GB002797, 2007.

Wang, Y.-P. P., Law, R. M., and Pak, B.: A global model of carbon, nitrogen and phosphorus cycles for the terrestrial biosphere, Biogeo-
15 sciences, 7, 2261–2282, doi:10.5194/bg-7-2261-2010, 2010.

Wieder, W. R., Cleveland, C. C., Lawrence, D. M., and Bonan, G. B.: Effects of model structural uncertainty on carbon cycle projections: biological nitrogen fixation as a case study, Environ. Res. Lett., 10, 044 016, doi:10.1088/1748-9326/10/4/044016, http://stacks.iop.org/1748-9326/10/i=4/a=044016?key=crossref.27ff2d3c016ebe5e184f5d9334a5791f, 2015.

Yang, X. and Post, W. M.: Phosphorus transformations as a function of pedogenesis: a synthesis of soil phosphorus data using Hedley fraction-
20 ation method, Biogeosciences, 8, 5907–5934, doi:10.5194/bgd-8-5907-2011, http://www.biogeosciences-discuss.net/8/5907/2011/http://www.biogeosciences.net/8/2907/2011/, 2011.

Yang, X., Post, W. M., Thornton, P. E., Jain, A., and Ridge, O.: The distribution of soil phosphorus for global biogeochemical modeling, pp. 2525–2537, doi:10.5194/bg-10-2525-2013, 2013.

Yang, X., Thornton, P. E., Ricciuto, D. M., and Post, W. M.: The role of phosphorus dynamics in tropical forests - A modeling study using
25 CLM-CNP, Biogeosciences, 11, 1667–1681, doi:10.5194/bg-11-1667-2014, http://www.biogeosciences.net/11/1667/2014/, 2014.

Zaehle, S. and Friend, A. D.: Carbon and nitrogen cycle dynamics in the O-CN land surface model: 1. Model description, site-scale evaluation, and sensitivity to parameter estimates, Global Biogeochem. Cycles, 24, 1–13, doi:10.1029/2009GB003521, 2010.

Zaehle, S., Ciais, P., Friend, A. D., and Prieur, V.: Carbon benefits of anthropogenic reactive nitrogen offset by nitrous oxide emissions, Nat. Geosci., 4, 601–605, doi:10.1038/ngeo1207, http://dx.doi.org/10.1038/ngeo1207, 2011.

30 Zaehle, S., Medlyn, B. E., Kauwe, M. G. D., Walker, A. P., Dietze, M. C., Hickler, T., Luo, Y., Wang, Y.-p., El-masri, B., Thornton, P., Jain, A., Wang, S., Warlind, D., Weng, E., Parton, W., Iversen, C. M., Gallet-budynek, A., Mccarthy, H., Finzi, A. C., Hanson, P. J., Prentice, I. C., Oren, R., and Norby, R. J.: Evaluation of 11 terrestrial carbon – nitrogen cycle models against observations from two temperate Free-Air CO 2 Enrichment studies, New Phytol., 202, 803–822, doi:10.1111/nph.12697, 2014.

Zhang, Z., Rengel, Z., and Meney, K.: Kinetics of ammonium, nitrate and phosphorus uptake by Canna indica and Schoenoplectus validus,
35 Aquat. Bot., 91, 71–74, doi:10.1016/j.aquabot.2009.02.002, 2009.